Corrected and Republished from: The COP9 Signalosome Interacts with and Regulates Interferon Regulatory Factor 5 Protein Stability

Justyna Korczeniewska,[a,b] Betsy J. Barnes[a,b]

[a]Department of Biochemistry & Molecular Biology, New Jersey Medical School, UMDNJ, Newark, New Jersey, USA

[b]New Jersey Medical School-University Hospital Cancer Center, UMDNJ, Newark, New Jersey, USA

PUBLISHER'S NOTE The American Society for Microbiology and *Molecular and Cellular Biology* would like to inform readers that this article is a corrected and republished version of one (https://doi.org/10.1128/MCB.00802-12) which was retracted (https://doi.org/10.1128/MCB.00477-17). The original article was found to have image duplications in Fig. 2, 5, 6, and 7. Most of the duplications occurred in loading controls, such as β-actin and GAPDH, but were not limited to this. Owing to the number of figures affected, a correction was not allowed and the article was retracted. However, the authors were able to provide the original data that supported the results and conclusions presented in the article. Therefore, the authors were allowed to submit a revised manuscript for consideration.

ABSTRACT The transcription factor interferon regulatory factor 5 (IRF5) exerts crucial functions in the regulation of host immunity against extracellular pathogens, DNA damage-induced apoptosis, death receptor signaling, and macrophage polarization. Tight regulation of IRF5 is thus warranted for an efficient response to extracellular stressors and for limiting autoimmune and inflammatory responses. Here we report that the COP9 signalosome (CSN), a general modulator of diverse cellular and developmental processes, associates constitutively with IRF5 and promotes its protein stability. The constitutive CSN/IRF5 interaction was identified using proteomics and confirmed by endogenous immunoprecipitations. The CSN/IRF5 interaction occurred on the carboxyl and amino termini of IRF5; a single internal deletion (Δ455-466) was found to significantly reduce IRF5 protein stability. CSN3 was identified as a direct interacting partner of IRF5, and knockdown of this subunit with small interfering RNAs (siRNAs) resulted in enhanced degradation. Degradation was further augmented by knockdown of CSN1 and CSN3 together. The ubiquitin E1 inhibitor UBEI-41 or the proteasome inhibitor MG132 prevented IRF5 degradation, supporting that its stability is regulated by the ubiquitin-proteasome system. Importantly, activation of IRF5 by the death receptor ligand tumor necrosis factor (TNF)-related apoptosis-inducing ligand (TRAIL) resulted in enhanced degradation via loss of the CSN/IRF5 interaction. This study defines the CSN as a new interacting partner of IRF5 that controls its stability.

KEYWORDS COP9, IRF5

The interferon regulatory factor (IRF) family consists of nine cellular IRFs, each with pleiotropic biological functions (1). IRF5 has an important role in the induction of type I interferons (IFNs) and proinflammatory cytokines and is thus a critical mediator of innate and adaptive immunity (2–4). More recent studies have shown that *Irf5* is an autoimmune susceptibility gene associated with increased risk of

human systemic lupus erythematosus (SLE), rheumatoid arthritis (RA), and Sjögren's syndrome (5–9). In addition to being one of the key factors mediating MyD88-dependent Toll-like receptor (TLR) signaling, mouse and human cells lacking *Irf5* are resistant to undergoing DNA damage- or death receptor-induced apoptosis, supporting a critical role for IRF5 in the cellular response to a variety of extracellular stressors (10–14). To this extent, loss of IRF5 expression in both mouse and human cells has recently been shown to contribute to tumorigenesis and metastasis (4, 10, 14, 15).

IRF5 is a latent transcription factor that is constitutively expressed in most hematopoietic cells and can be upregulated in many other cell types in response to type I IFNs or DNA damage (2, 10, 14, 16, 17). IRF5 resides in the cytoplasm of most unstimulated cells and becomes activated by posttranslational modifications that include phosphorylation, acetylation, and/or ubiquitination, resulting in translocation to the nucleus (2, 13, 18–22). While all IRF family members share significant homology in their amino-terminal DNA binding domain (DBD), the carboxyl terminus of individual IRFs is not well conserved and thus is thought to dictate specific interactions with other proteins and IRF family members that control/mediate their distinct functions (1, 21). Little is still known of IRF5-interacting partners. We and others and have identified a few proteins that interact with IRF5, including IRF1, IRF3, IRF7 (23), CBP/p300, histone deacetylases (5, 21), TRAF6, MyD88, IRAK1, and IRAK4 (3, 18). The exact functional consequences of each of these interactions have not been fully elucidated, but most are thought to be associated with IRF5 activation.

In the current study, we identified the constitutive photomorphogenesis 9 (COP9) signalosome as a new interacting partner of IRF5 in unstimulated cells. The COP9 signalosome (CSN) is a highly conserved protein complex that consists of eight subunits known as CSN1 to CSN8 (24, 25). The complex was first discovered in *Arabidopsis* as a suppressor of light-dependent growth (26–28), and subsequent work identified and characterized the CSN in mammals (24, 25), yeast (29), fungi (30), and *Caenorhabditis elegans* (31), highlighting its role as a general modulator of diverse cellular and developmental processes. The most well-studied function of the CSN is its regulation of protein degradation, and research in a variety of organisms has supported the notion that the CSN is biochemically linked to the ubiquitin-proteasome pathway (32–37). Equally interesting and potentially important to the regulation of IRF5 function is the ability of the CSN to act as a scaffold to control/mediate phosphorylation of transcriptional regulators through the activity of CSN-associated kinases (reviewed in reference 38). Kinase signaling and ubiquitin-mediated protein degradation are generally not mutually exclusive, and phosphorylation often regulates protein degradation. The CSN has also been shown to regulate the subcellular localization of different signaling molecules (39, 40).

The goal of the present study was to characterize the functional consequence of this newly identified CSN/IRF5 interaction in unstimulated cells and to determine how the resulting function may be altered in response to a stimulus that induces IRF5 activation. Collectively, we found that the CSN/IRF5 interaction controls IRF5 protein stability via interaction with both the carboxyl and amino termini of IRF5. Loss of the CSN/IRF5 interaction resulted in enhanced degradation that was mediated by the ubiquitin-proteasome pathway and further enhanced by tumor necrosis factor (TNF)-related apoptosis-inducing ligand (TRAIL)-induced IRF5 activation.

RESULTS

Interaction of COP9 subunits with IRF5. To identify proteins that interact with IRF5, a proteomics-based approach was used. A plasmid encoding the full-length Flag-tagged IRF5 variant 3/4 was transiently transfected into Hek 293T cells that otherwise lack endogenous IRF5. Proteins that immunoprecipitated with anti-Flag antibodies (IRF5) were resolved by one-dimensional sodium dodecyl sulfate-polyacrylamide gel electrophoresis (SDS-PAGE) and stained with SYPRO ruby, and bands were cut and identified by mass spectrometry (MS) analysis. In addition to confirming the presence of high levels of ectopic Flag-tagged IRF5 at ~60 kDa in
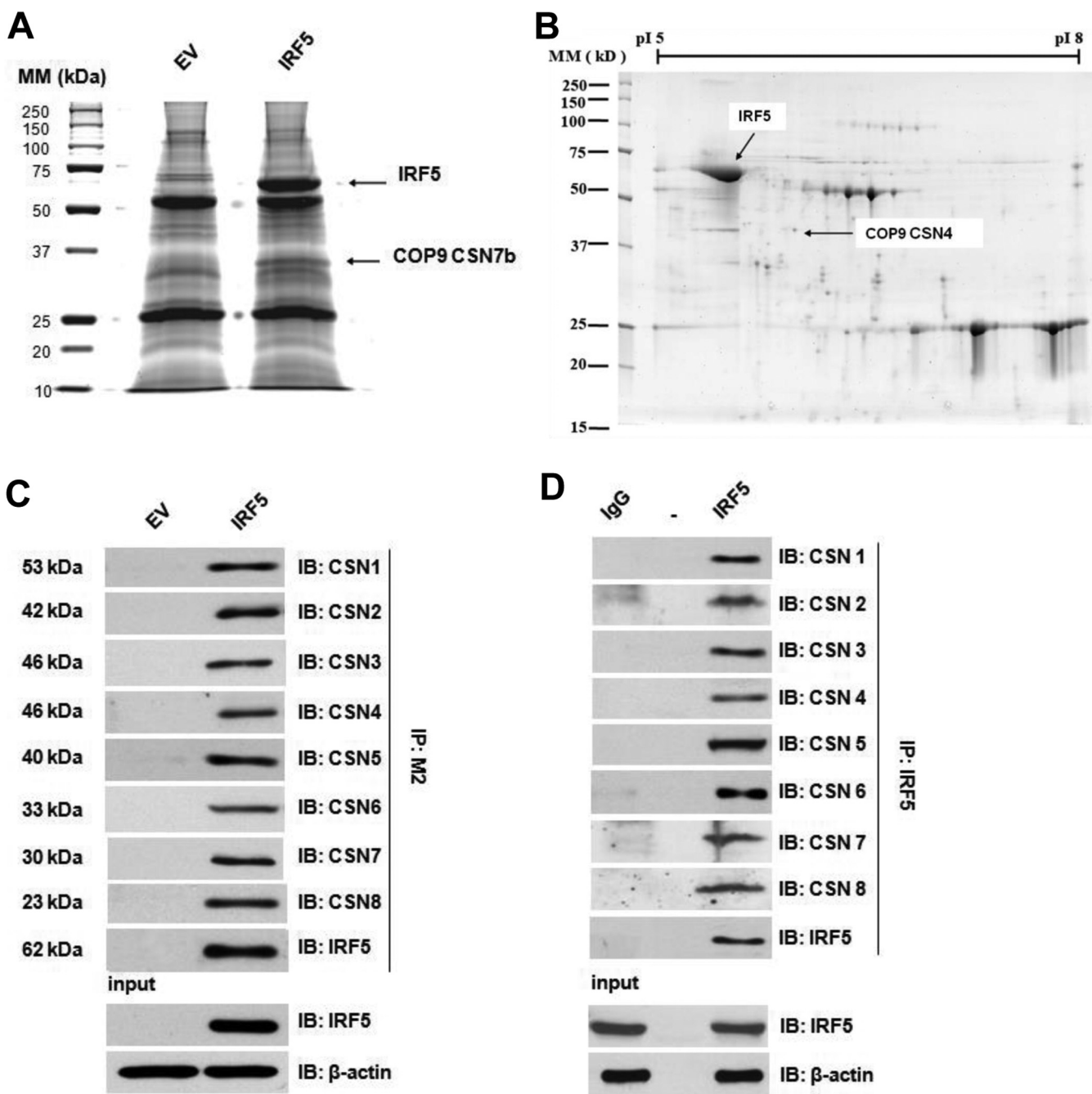
FIG 1 Identification of the COP9 signalosome as a novel interacting partner of IRF5. (A) Representative gel image from the transient transfection of Flag-tagged IRF5 (IRF5) or empty Flag-tagged vector control (EV) to Hek 293T cells. Lysates were immunoprecipitated with anti-Flag M2 antibodies, and proteins bound to beads were separated by SDS-PAGE. Proteins were stained with SYPRO ruby, and the indicated bands were excised for LC/MS-MS analysis. The molecular mass (MM) marker is shown on the left. (B) Same as that described for panel A except that immunoprecipitated lysates were separated by 2-D gel electrophoresis. A representative gel image from cells overexpressing Flag-tagged IRF5 is shown. The gel was stained with SYPRO ruby, and the indicated spots that were unique to cells expressing IRF5 compared to EV control cells were excised for LC/MS-MS analysis. (C) Same as that described for panel A except that resolved proteins were immunoblotted with antibodies specific for each COP9 subunit. The IRF5 input and loading control β-actin are shown. (D) Similar to that described for panel C except that THP-1 cells were immunoprecipitated with IgG isotype control antibodies or anti-IRF5 antibodies. COP9 subunits were identified by immunoblot analysis.

the IRF5-transfected cells, we identified another unique band at ~35 kDa that was not present in empty vector control cells (Fig. 1A). Analysis of this band by liquid chromatography-tandem MS (LC/MS-MS) revealed that it consisted primarily of the COP9 subunit 7 isoform b (gi 12232385) with a confidence interval of ≥95%. COP9 subunit 7 (CSN7) is the seventh subunit of the COP9 signalosome complex, which has

been shown to interact with Int6/eIF3, casein kinase 2 (CK2), and PMF-1 (41–43). CSN7 can itself be phosphorylated and can interact with kinases, supporting the idea that the CSN is a central component of kinase-mediated signal transduction pathways (24, 42, 44–46).

In a similar independent experiment whereby proteins that immunoprecipitated with anti-Flag antibodies were resolved by two-dimensional (2-D) gel electrophoresis in order to obtain more detailed insight into the proteins that may be interacting with IRF5, we were able to detect another COP9 subunit, CSN4, in the pulled-down precipitate (Fig. 1B). Little is known of CSN4 function in mammalian cells, yet CSN4 to CSN7 (CSN4-7) have previously been designated a mini-CSN subcomplex (47).

To confirm the interaction of IRF5 with the CSN, and to determine whether additional subunits could be detected as interacting with IRF5, we performed immunoprecipitation of Flag-tagged IRF5 in Hek 293T cells and immunoblotted resolved proteins with antibodies specific to each CSN subunit. We found that all CSN subunits could be pulled down in the cells overexpressing IRF5 and not empty vector control cells (Fig. 1C). To further confirm these interactions, we immunoprecipitated endogenous IRF5 from THP-1 cells, which express high levels of IRF5, and immunoblotted with individual CSN subunit antibodies. Similar to data in Fig. 1C, we detected a specific interaction of all subunits with IRF5, since these interactions were absent in THP-1 cells immunoprecipitated with anti-IgG control antibodies (Fig. 1D).

Mapping CSN binding to the amino and carboxyl termini of IRF5. We next mapped the domain of IRF5 responsible for interaction with the CSN. Like most IRF family members, IRF5 possesses a protein-interacting domain in its carboxyl terminus (Fig. 2A), so we focused on this region first for detection of CSN binding. A series of carboxyl-terminal deletion mutants were generated and transiently transfected individually to Hek 293T cells, and lysates were immunoprecipitated with anti-Flag antibodies. Binding of endogenous CSN subunits to Flag-tagged IRF5 was determined by immunoblotting with anti-CSN subunit-specific antibodies. Construct 1-489, representing full-length IRF5 (comprising amino acids [aa] 1 to 489), and consecutively shorter constructs 1-477, 1-411, 1-326, and 1-246 were tested for their interaction with CSN subunits. Interaction of individual subunits with full-length IRF5 and the 1-477 deletion mutant was detected (Fig. 2B); interaction was absent in the shorter constructs, indicating that CSN subunits interact between aa 411 to 477 of IRF5. Consecutively shorter mutants were generated in this region, and a distinct loss of interaction was observed between aa residues 433 to 444 and 455 to 466 (Fig. 2C). The altered binding pattern between aa 422 and 466 may reflect true interactions or may be an artifact of the entire three-dimensional structure of IRF5 changing due to the large deletions at the carboxyl terminus. To address whether both of these regions are essential for interaction with the CSN, we generated Δ433-444 and Δ455-466 internal deletion mutants for immunoprecipitation experiments. We found that only the mutant lacking aa 455 to 466 was incapable of interacting with the CSN (Fig. 2D).

In a similar manner, we examined the ability of the CSN to interact with the amino-terminal DNA binding domain of IRF5. In previous work, we had identified a carboxyl-terminal autoinhibitory domain (AID) of IRF5 that was proposed to mask the amino-terminal DNA binding domain in unstimulated cells, supporting a closed structure for inactive IRF5 monomers (19). Subsequent crystallography data supported the presence of a functional IRF5 AID that masks the DNA binding domain in unstimulated cells (48). Similar to the carboxyl-terminal mapping, a number of amino-terminal deletion mutants were generated and analyzed for interaction with CSN subunits (data not shown). Eventually, the region interacting with the CSN was narrowed down to aa 41 to 50 (Fig. 2E). Taking into account data from the carboxyl-terminal IRF5 internal deletion mutants (Fig. 2D), we found that both regions (aa 41 to 50 and 455 to 466) are required for interaction of IRF5 with the CSN and support a folded conformation whereby the carboxyl terminus of IRF5 is folded over the amino-terminal DNA binding domain.
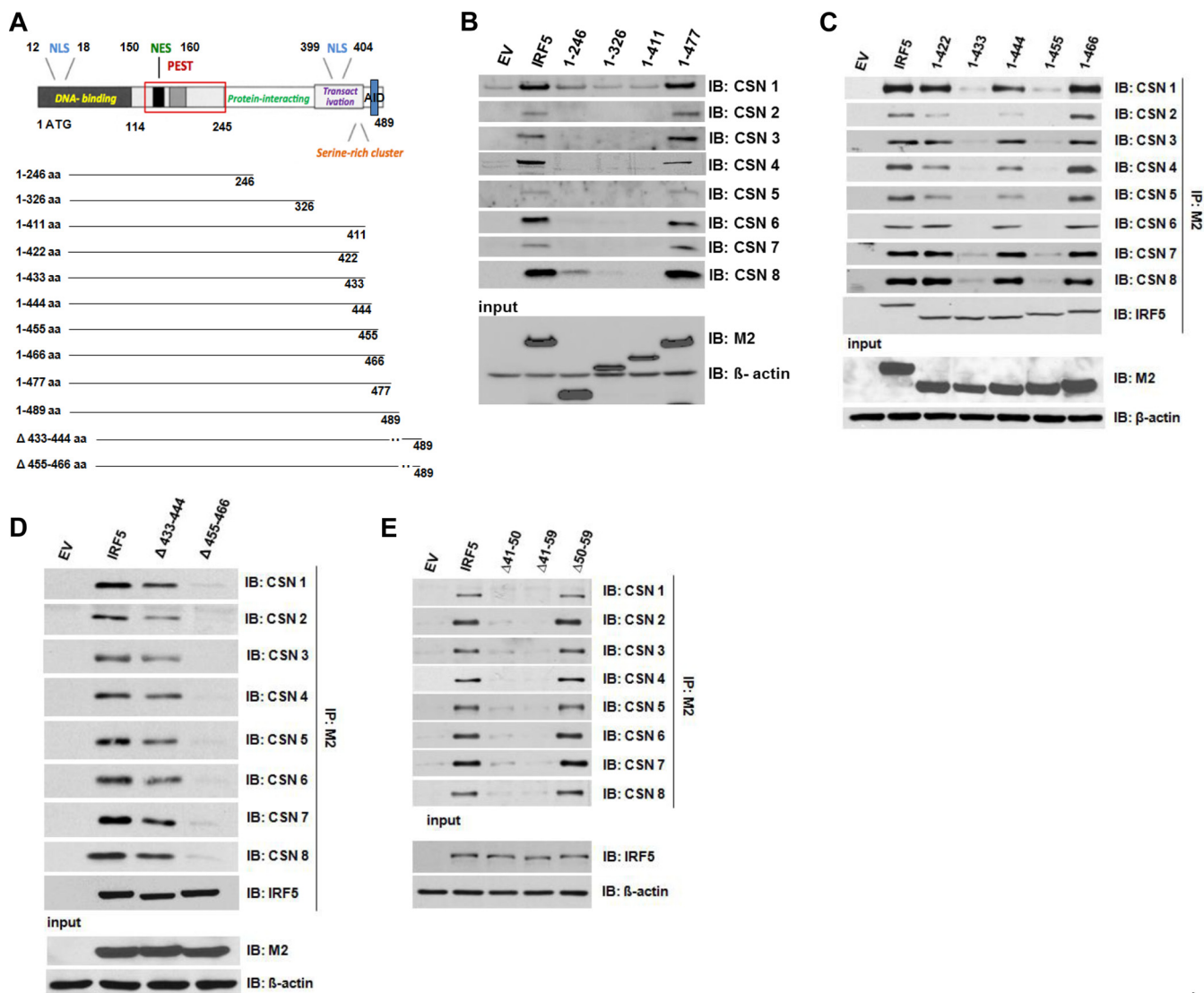
FIG 2 The CSN interacts with the amino and carboxyl termini of IRF5. (A) Scheme of the IRF5 protein structure with functional domains and newly generated carboxyl-terminal deletion mutants. NLS, nuclear localization signal; NES, nuclear export signal; PEST, region rich in proline (P), glutamic acid (E), serine (S), and threonine (T) residues; AID, autoinhibitory domain. (B) Full-length Flag-tagged IRF5 and the indicated carboxyl-terminal deletion mutant plasmids were transiently transfected into Hek 293T cells and immunoprecipitated with anti-IRF5 antibodies, and binding of CSN subunits to IRF5 was detected by immunoblotting with antibodies specific to each subunit. Input lysates from each transfection are shown at the bottom with β-actin levels that serve as a loading control. (C) Same as that described for panel B except that additional carboxyl-terminal deletion mutants were generated and tested for their ability to interact with COP9 subunits. (D) The CSN interacts with IRF5 between aa 455 and 466. Same as that described for panels B and C except that internal deletion mutants of IRF5 were transiently transfected into Hek 293T cells. (E) Same as that described for panel D except that amino-terminal IRF5 internal deletion mutants were transiently transfected into Hek 293T cells and interaction with individual COP9 subunits was determined by immunoblotting.

We next sought to determine which subunit(s) might be interacting directly with IRF5. Using the TNT quick coupled transcription/translation assay, we generated cell-free recombinant IRF5, CSN2, CSN3, and CSN5 proteins for coimmunoprecipitation experiments. All four proteins were produced at a high yield, and equal amounts of IRF5 were coincubated with equal amounts of each CSN subunit; only CSN3 was detected as interacting directly with IRF5 (Fig. 3).

CSN controls IRF5 protein stability. Given that the interaction between IRF5 and the CSN occurs in unstimulated cells, combined with the fact that the most well-studied function of the CSN is regulation of protein stability, we postulated that this interaction might control IRF5 stability. Little to nothing is known of IRF5 protein stability. We previously identified a large PEST domain in the IRF5 protein sequence (illustrated in Fig. 2A) and hypothesized that it would control IRF5 protein stability (19). The PEST
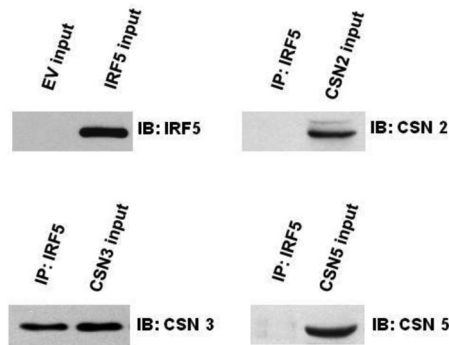
FIG 3 COP9 subunit 3 directly interacts with IRF5. Cell-free recombinant IRF5, CSN2, CSN3, and CSN5 proteins were generated using the TNT quick coupled transcription/translation assay for coimmunoprecipitation experiments. Western blot analysis of the four proteins shows input for each coimmunoprecipitation; equal amounts of IRF5 were used in each assay. Only the interaction of CSN3 with IRF5 was detected after immunoprecipitating for IRF5.

domain is a region rich in proline (P), glutamic acid (E), serine (S), and threonine (T) residues and is thought to target proteins for proteolytic degradation. However, recent data from our laboratory indicate that the PEST domain has little to do with IRF5 protein stability since the IRF5 isoform V5, which contains an intact PEST domain, is significantly more stable than V8, which lacks the entire PEST domain (17, 19, 86). These data support that additional mechanisms that control IRF5 protein stability exist.

To determine whether the CSN/IRF5 interaction controls IRF5 protein stability, we compared the stability of full-length IRF5 proteins with that of IRF5 proteins encoded by the Δ455-466 mutant by cycloheximide (CHX) chase. Full-length Flag-tagged IRF5 and Δ455-466 plasmids were transiently transfected into Hek 293T cells and left untreated or treated with CHX over a time course; protein levels were analyzed by immunoblotting with anti-Flag antibodies. Data in Fig. 4A indicate enhanced degradation of IRF5 proteins lacking the CSN interaction domain between aa 455 and 466; data in Fig. 4B, from parallel untreated samples, indicate the specificity of CHX treatments. To obtain more quantitative insight into the CSN's control of IRF5 protein stability/ degradation, we used a modified CHX chase technique whereby Hek 293T cells, transiently transfected with green fluorescence protein (GFP)-tagged full-length IRF5 or the Δ455-466 mutant, were fractionated by fluorescence-activated cell sorting (FACS) into subpopulations expressing "low," "medium," and "high" levels of GFP. Only the medium level-expressing cells, shown to be the most sensitive to CHX (49), were subjected to CHX treatment. The absolute slope of decreasing mean fluorescence intensity (MFI) over time (reflecting relative half-life and stability) was determined. Full-length GFP-IRF5 had the smallest decrease in MFI over time and therefore a smaller absolute slope, while the Δ455-466 mutant had the larger decrease in MFI and a steeper slope (Fig. 4C). Representative histogram plots of fluorescence distribution and gating are shown for the full-length and mutant proteins, revealing similar distributions (Fig. 4D). These data support findings from immunoblot analysis showing that the IRF5 Δ455-466 mutant degrades faster than full-length IRF5. Comparable data were obtained by standard flow cytometric analysis of total IRF5 expression after treatment of cells with CHX (Fig. 4E and F). Both sets of flow cytometric data gave a significant difference between the absolute slopes of full-length IRF5 and the Δ455-466 construct, indicating that loss of the CSN interaction significantly decreases IRF5 protein stability (Fig. 4C and E). As a positive control, the ability of GFP-IRF5 fusion proteins to interact with COP9 subunits was tested by immunoprecipitation; similar to their Flag-tagged counterparts, full-length GFP-IRF5 interacted with all COP9 subunits while the GFP-tagged Δ455-466 mutant was unable to interact (Fig. 2 and 4G).

Knockdown of CSN1 and CSN3 promotes IRF5 degradation. It has previously been shown that downregulation of CSN1 and CSN3 by specific small interfering RNAs
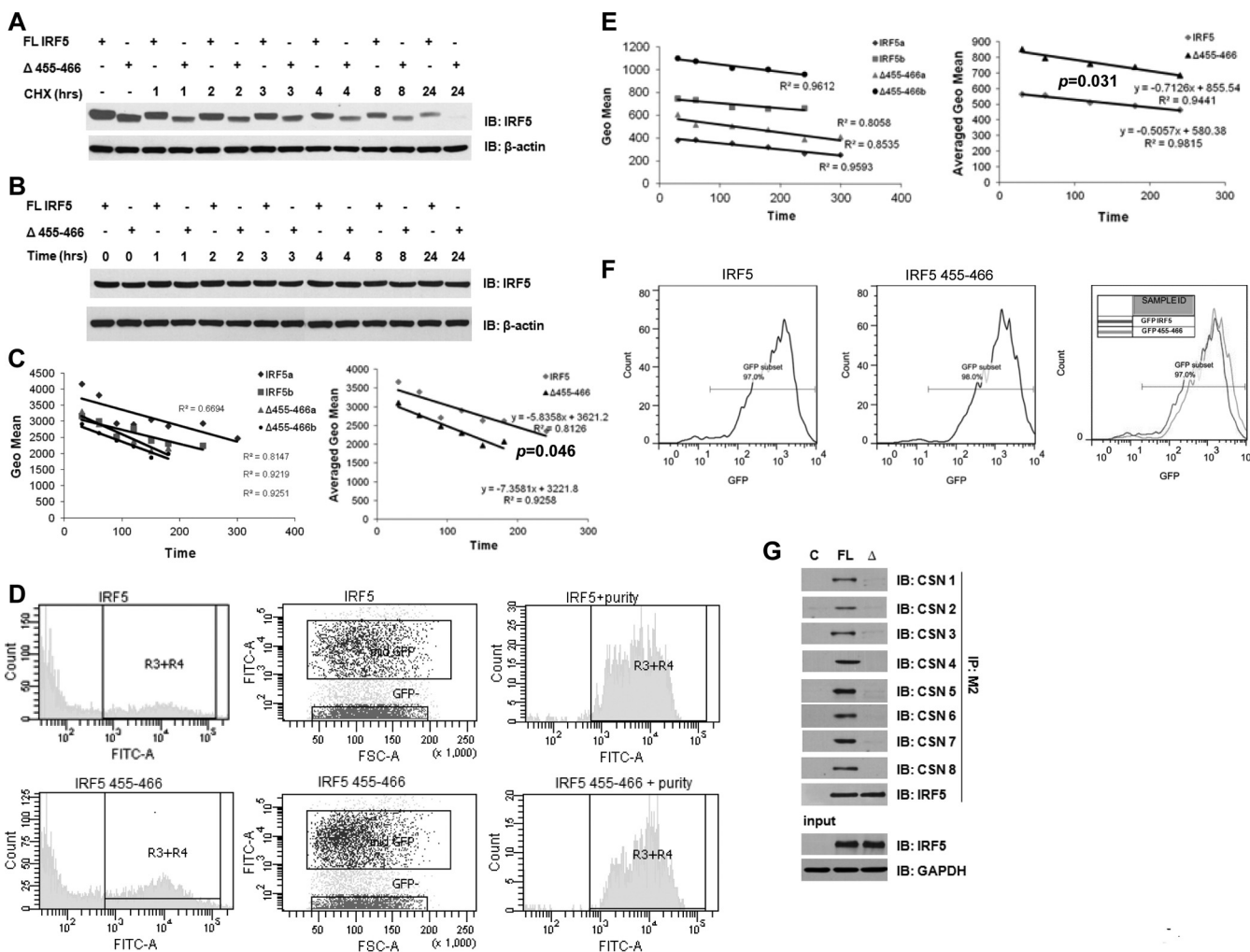
FIG 4 CSN/IRF5 interaction controls IRF5 protein stability. (A) Plasmids encoding full-length (FL) and mutant (Δ455-466) Flag- or GFP-tagged IRF5 were transiently transfected into Hek 293T cells and chased with cycloheximide (CHX). Cells were harvested at the indicated time points post-CHX treatment, and proteins were separated by SDS-PAGE. Protein levels were determined by immunoblot (IB) analysis with anti-IRF5 and anti-β-actin antibodies. (B) Same as that described for panel A except that cells were left untreated and harvested at each indicated time point. (C) Cells expressing medium levels of GFP-IRF5 were sorted and treated with CHX for the indicated time periods and then gated on by flow cytometry to determine the intracellular levels of IRF5. GFP intensity was quantified at each time point and plotted on a graph as a function of time. The rate of exogenous protein decay was determined by fitting a line to each data set and calculating the slope. Representative results from two independent replicates are shown (IRF5a and b; Δ455-466a and b); the average rate of decay was calculated from three independent experiments performed in duplicate. $P < 0.05$ by paired two-tailed Student t test. (D) Representative histograms of fluorescence distribution and sorting of cells expressing medium (R3+R4) levels of GFP-tagged full-length and mutant IRF5 proteins. The purity of sorted cells that were treated with CHX is shown. (E) Same as that described for panel C except that the total cells transfected with either plasmid were treated with CHX over the indicated time periods and IRF5 levels were determined by flow cytometry. (F) Same as that described for panel D except that representative histograms show the strategy of gating on GFP-IRF5-positive cells. The geometric mean was obtained from the subset of cells indicated in the fluorescence histograms. An overlay of the two experimental conditions is shown. (G) Full-length (FL) and mutant (Δ) GFP-IRF5 proteins were transiently transfected into Hek 293T cells, lysates were immunoprecipitated with anti-IRF5 antibodies, and the interaction with individual COP9 subunits was determined by immunoblotting.

(siRNAs) targeting these two subunits leads to an approximately 40% reduction of the subunits and a proportional reduction of the entire CSN complex (50). Since we have found that CSN3 interacts directly with IRF5 (Fig. 3), we examined the effect of targeting CSN3 or both subunits (CSN1 and CSN3) on IRF5 protein stability. Specific siRNAs targeting each of these subunits were transiently cotransfected into Hek 293T cells with plasmids encoding full-length Flag-tagged IRF5 or the Δ455-466 mutant and treated with CHX over a time course. Expression of IRF5 and the subunits was determined by immunoblot analysis (Fig. 5A). Similar to what was observed in Fig. 4A, IRF5 Δ455-466 proteins degraded more rapidly than full-length IRF5 even in the presence of control siRNAs (Ctr siRNA); no effect of the control siRNAs on IRF5, CSN1, CSN3, or GAPDH (glyceraldehyde-3-phosphate dehydrogenase) expression was observed. Although
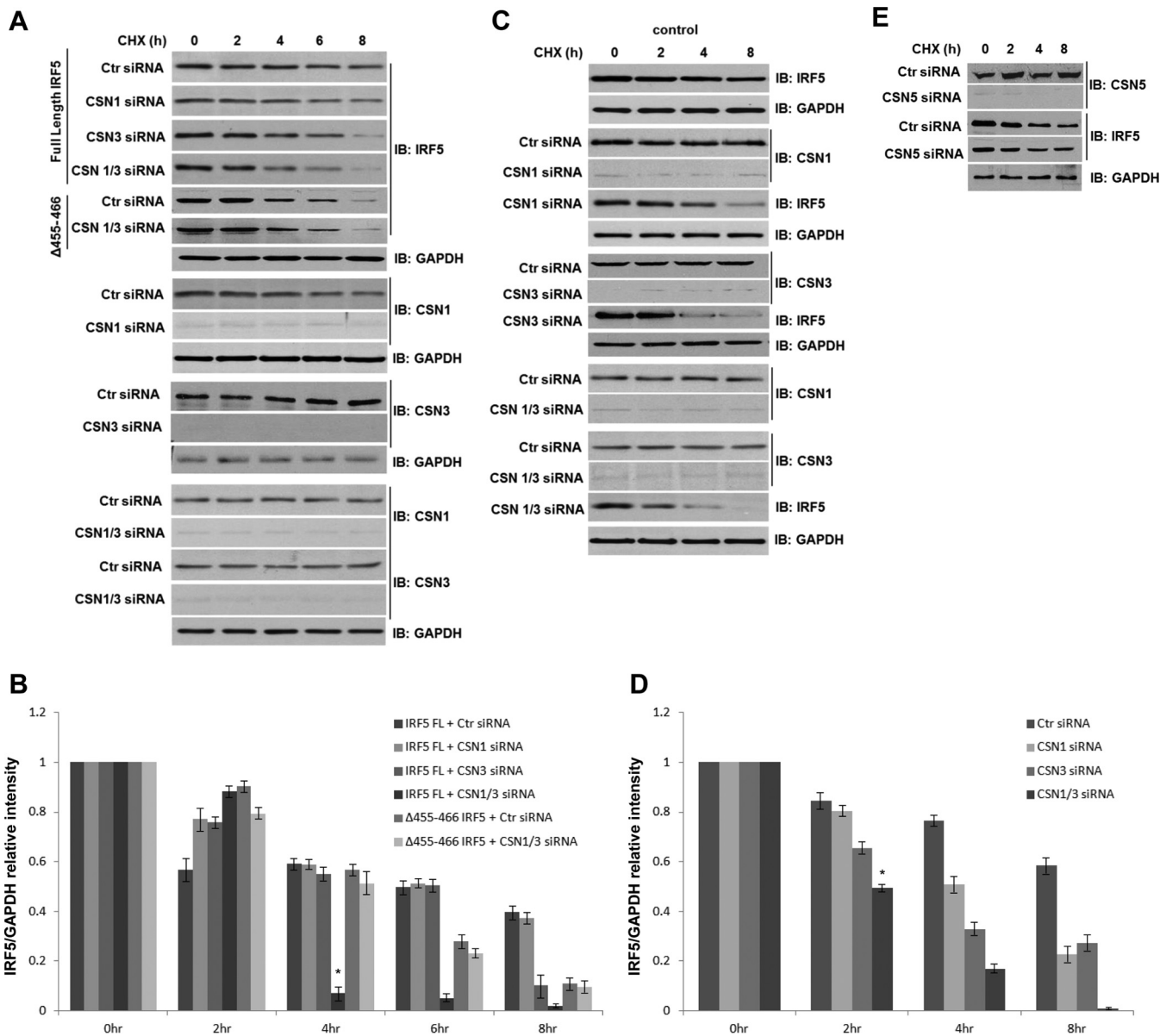
FIG 5 Knockdown of CSN1 and CSN3 promotes IRF5 degradation. (A) Plasmids encoding full-length (FL) IRF5 or the Δ455-466 mutant were transiently cotransfected with control siRNAs (Ctr siRNA) or siRNAs targeting CSN1, CSN3, or the combination of the two, into Hek 293T cells. Cells were then treated with CHX, and protein expression was analyzed over the indicated time periods post-CHX treatment. Knockdown efficiency for each siRNA is shown for each independent transfection; GAPDH levels are shown as an internal loading control. Representative data from three independent experiments are shown. (B) Quantitation of IRF5 expression from panel A after densitometry analysis using ImageJ software; means ± SD are plotted from three independent experiments. The point at which the effect of the CSN1/3 knockdown on IRF5 FL stability becomes statistically significant is shown; *, $P < 0.001$ by Student's t test. (C) Same as that described for panel A except that siRNAs were transiently transfected into THP-1 cells and endogenous IRF5 and CSN subunits 1 and 3 were examined by immunoblotting with specific antibodies. Representative data from three independent experiments are shown. (D) Same as that described for panel B except that relative IRF5 expression from panel C is quantified; means ± SD are plotted from three independent experiments. The point at which the effect of the CSN1/3 knockdown on IRF5 stability becomes statistically significant is shown; *, $P < 0.01$ by Student's t test. (E) Same as that described for panel C except that siRNAs targeting CSN5 were transfected into THP-1 cells and their effect on IRF5 expression was examined. Representative data from three independent experiments are shown.

nearly 100% knockdown of CSN1 and CSN3 expression was achieved, little effect of the CSN1 knockdown on IRF5 expression was observed, while knockdown of CSN3 on its own achieved a dramatic decrease in IRF5 expression at 8 h. Interestingly, knockdown of both CSN1 and CSN3 at the same time gave a degradation pattern for full-length IRF5 similar to that seen with the Δ455-466 mutant. As expected, knockdown of both CSN1 and CSN3 in cells expressing IRF5 Δ455-466 proteins had no effect on degradation. Quantitation of these data is shown in Fig. 5B.

Similar data were obtained when CSN siRNAs were transiently transfected into THP-1 cells and endogenous IRF5 protein levels were examined after treatment of cells with CHX (Fig. 5C). In this experiment, knockdown of CSN1 by itself gave a reduction in IRF5 levels at 8 h post-CHX treatment and CSN3 knockdown resulted in an even more rapid decay of IRF5 proteins that occurred between 2 and 4 h post-CHX treatment. The combined knockdown of CSN1 and CSN3 was the most effective in reducing IRF5 protein stability. Quantitation is shown in Fig. 5D. As a negative control, we examined whether knockdown of another COP9 subunit, CSN5, which does not directly interact with IRF5 (Fig. 3) or affect the CSN complex (50), would have an effect on IRF5 stability. Data in Fig. 5E demonstrate that loss of CSN5 has no effect on IRF5 degradation. Together, these data support a clear and important role for CSN3 and the entire CSN complex in regulating IRF5 protein stability.

IRF5 degradation is regulated by the ubiquitin-proteasome pathway. One of the best-characterized functions of the CSN is the control of proteolysis via the ubiquitin-proteasome pathway (34). Ubiquitylation is catalyzed by the sequential action of ubiquitin-activating enzyme (E1), ubiquitin-conjugating enzyme (E2), and a ubiquitin protein ligase (E3). Ubiquitylation is essential to numerous cellular and developmental processes, including, but not limited to, protein quality control, growth, apoptosis, antigen presentation, DNA repair, and signal transduction (42, 51–57). The most well-characterized role for ubiquitin is in targeting proteins for degradation by the 26S proteasome after modification with chains of four or more ubiquitins. To test whether CSN-dependent stabilization of IRF5 is due to altered recognition of IRF5 by the ubiquitin-proteasome pathway, Hek 293T cells expressing full-length IRF5 or the Δ455-466 mutant were treated with the E1 ubiquitin inhibitor UBEI-41 or the proteasome inhibitor MG132 in conjunction with CHX. E1 inhibitors target the common first step in ubiquitylation, and MG132 targets the final destination for many ubiquitylated proteins. The rate of IRF5 protein decay was measured by immunoblot analysis. Consistent with the data in Fig. 4 and 5, the observed reduction in full-length IRF5 protein levels over time after treatment of cells with CHX was greatly enhanced in the mutant lacking the ability to interact with the CSN (Fig. 6A). However, treatment of full-length or Δ455-466 IRF5-expressing cells with UBEI-41 or MG132 protected IRF5 from degradation (Fig. 6A). This effect was specific for IRF5, as no change in GAPDH protein levels was observed. These results suggest that the CSN/IRF5 interaction protects IRF5 from ubiquitination and degradation by the 26S proteasome pathway.

IRF5 undergoes K48-linked ubiquitination in the absence of the CSN/IRF5 interaction. The most abundant polyubiquitin chains in living cells are K48 linkages, which adopt a closed conformation and serve as a signal for target protein degradation by the 26S proteasome. The next most common are K63 linkages that adopt an extended linear conformation as nonproteasome recognizing and often lead to the activation of signaling functions. To this extent, it has previously been shown that IRF5 undergoes TRAF6-mediated K63-linked ubiquitination when IRF5, MyD88, and TRAF6 are overexpressed in Hek 293 cells (18). The TRAF6-mediated K63-linked ubiquitination of IRF5 led to its nuclear translocation and enhanced transactivation potential (18). Based on these findings and the new data in Fig. 6A suggesting that IRF5 becomes ubiquitinated when it is unable to interact with the CSN, we examined IRF5 ubiquitination in Hek 293T cells cotransfected with hemagglutinin-ubiquitin (HA-Ub) and full-length IRF5 or the Δ455-466 mutant. It was not surprising that we detected polyubiquitination of the Δ455-466 mutant and not of full-length IRF5 (Fig. 6B). Using an antibody that specifically recognizes K48-linked ubiquitination, we were able to characterize the polyubiquitination as K48 linked. These data support the premise that the interaction of IRF5 with the CSN protects it from undergoing K48-linked ubiquitination and degradation by the 26S proteasome pathway.

Activation of IRF5 by TRAIL enhances degradation. It is well known that many proteins that become phosphorylated in response to a given stimuli are subsequently ubiquitinated, followed by proteasome-dependent degradation (32, 44). IRF5 is
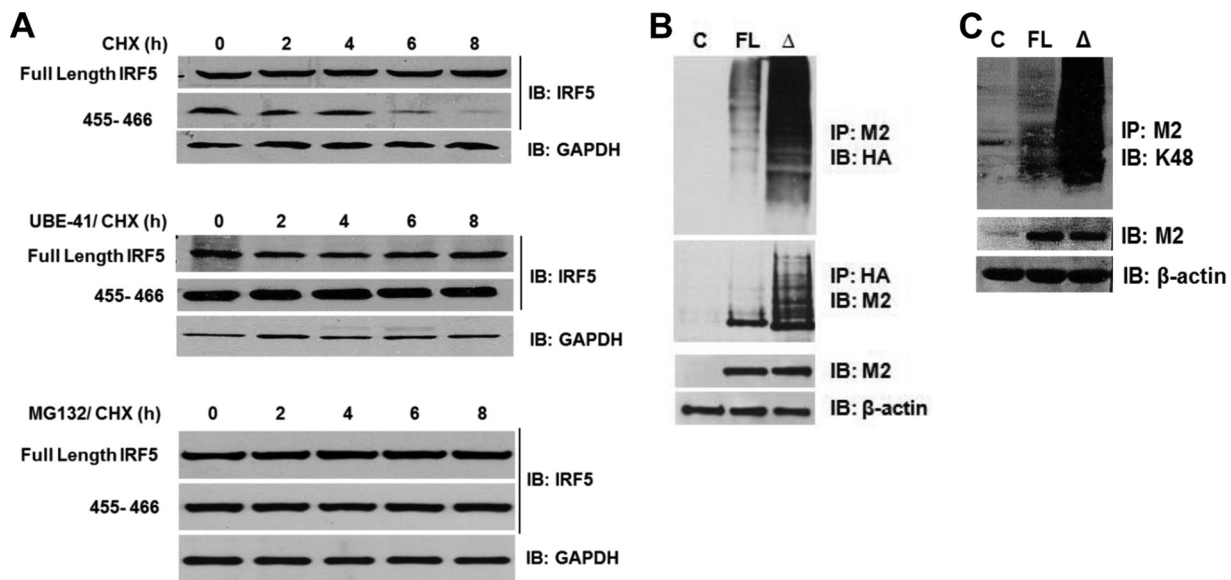
FIG 6 IRF5 degradation is abrogated by the inhibition of ubiquitin activating enzyme 1 (E1) or the proteasome. (A) Plasmids encoding full-length IRF5 or the Δ455-466 mutant were transiently transfected into Hek 293T cells and treated with CHX or CHX plus UBE-41 (ubiquitin E1 inhibitor) or MG132 (proteasome inhibitor). The rate of IRF5 and GAPDH protein decay was examined by immunoblot analysis. Panels are labeled by treatment regimen. (B) Similar to that described for panel A except that the HA-Ub plasmid was cotransfected with plasmids encoding empty vector (lane C), full-length IRF5 (lane FL), or Δ455-466 mutant IRF5 (lane Δ) into Hek 293T cells to examine IRF5 ubiquitination. Reciprocal immunoprecipitations are shown by pulling down IRF5 (M2) or ubiquitin (HA). Levels of IRF5 and β-actin are shown in whole-cell lysates used for immunoprecipitations. (C) Similar to that described for panel B except that cells were not transfected with HA-Ub and the levels of IRF5 K48-linked ubiquitination were determined by immunoblotting M2 precipitates with anti-K48-linked polyubiquitination antibodies. Expression of IRF5 and β-actin in whole-cell lysates used for the immunoprecipitations is shown.

thought to be activated by phosphorylation in response to different extracellular stimuli, including virus, DNA damage, MyD88-dependent TLR ligands, and the death receptor ligand TRAIL (2, 3, 12, 13, 19, 20, 58), resulting in its biological activity. In order to test the functional significance of the CSN/IRF5 interaction in a cellular system known to activate endogenous IRF5 via phosphorylation of serine (Ser), threonine (Thr), and tyrosine (Tyr) residues (12), we treated THP-1 cells with TRAIL and examined whether IRF5 activation had any effect on its degradation. To begin these studies, we first confirmed that TRAIL could induce endogenous IRF5 nuclear localization. In our first study, while we were able to examine endogenous IRF5 phosphorylation, the appropriate reagents were not available to examine its endogenous cellular localization (12). We have recently optimized the use of imaging flow cytometry to examine endogenous IRF5 activation/nuclear localization in primary immune cells of patients with SLE (59). Using this same technology, we examined quantitatively the ability of TRAIL to induce endogenous IRF5 nuclear localization in THP-1 cells over time. Figure 7A shows representative images of cells costained with fluorescein isothiocyanate (FITC)-conjugated IRF5 and DRAQ5, a nuclear-specific stain. By examining similarity scores between DRAQ5 and IRF5 (as described in Materials and Methods), we found that >50% of cells staining positive for IRF5 had nuclear-localized IRF5 at 3 h poststimulation (Fig. 7B), confirming our previous results with ectopic GFP-tagged IRF5 (12). Using this 3-h time point as a surrogate indicator of TRAIL-induced IRF5 activation, i.e., phosphorylation, that triggers its nuclear accumulation, we next examined IRF5 protein stability in response to TRAIL after 4 h of treatment with CHX. In the absence of TRAIL, little change in IRF5 protein levels were observed at 4 h post-CHX treatment (Fig. 4A, 6, and 7C); however, in the presence of TRAIL and CHX, IRF5 degradation was readily observed, with no change in β-actin levels (Fig. 7C). Analysis of the CSN/IRF5 interaction by immunoprecipitation of THP-1 cells left untreated or treated with TRAIL over a time course revealed a time-dependent loss of the CSN/IRF5 interaction only in the cells treated with TRAIL (Fig. 7D). Together, these data support a physiological and func-
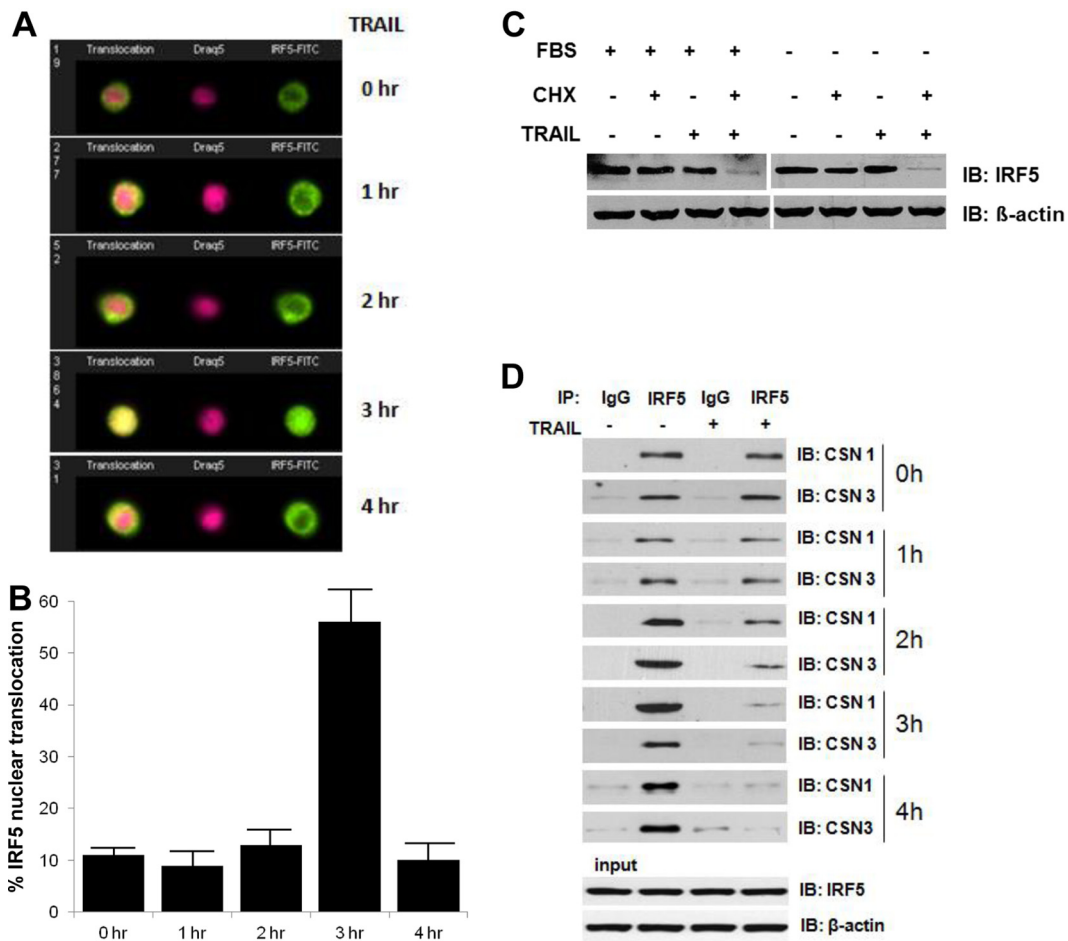
FIG 7 TRAIL triggers IRF5 nuclear localization and degradation due to loss of the CSN/IRF5 interaction. (A) THP-1 cells were treated with 25 ng/ml Superkiller TRAIL and intracellularly stained with FITC-conjugated IRF5 (green) and DRAQ5 (red). Representative single-cell images generated from IDEAS software are shown for each time point. (B) Graphic summary of endogenous IRF5 nuclear translocation in THP-1 cells after treatment with TRAIL. Data are representative of three independent experiments. Plotted values are the means ± SD. (C) TRAIL enhances IRF5 degradation. THP-1 cells were cultured under normal conditions with serum (FBS+) or without (serum starved; FBS−) and treated with CHX and/or Superkiller TRAIL for 4 h. Cells were harvested for immunoblot analysis of endogenous IRF5 and β-actin. (D) THP-1 cells were left untreated (−) or were treated (+) with Superkiller TRAIL over the indicated time course and then harvested for immunoprecipitation with anti-IRF5 antibodies (IP: IRF5) or nonspecific IgG control antibodies (IP: IgG). The interaction of IRF5 with CSN1 or CSN3 was determined by immunoblotting. Levels of IRF5 and β-actin in whole-cell lysates collected at the 4-h time point for immunoprecipitations are shown and are representative of what was found at all time points examined.

tional significance for the CSN/IRF5 interaction whereby activation/phosphorylation of IRF5 in response to TRAIL stimulation results in the enhanced degradation of IRF5 proteins due to loss of the CSN/IRF5 interaction.

Loss of the CSN/IRF5 interaction diminishes IRF5 transactivation potential. To determine whether the interaction of the CSN with IRF5 alters its transactivation potential, we compared the abilities of full-length and mutant IRF5 to transactivate an *ISRE*-containing luciferase reporter. Not surprising, given that the loss of the CSN/IRF5 interaction results in decreased IRF5 protein stability, we found that the Δ455-466 IRF5 mutant had decreased transactivation ability compared to that of full-length IRF5 (Fig. 8A). Since IRF5 is a critical mediator of TLR-induced proinflammatory cytokine expression, we also examined the abilities of full-length and mutant IRF5 to transactivate the *TNFA* promoter reporter after stimulation of Hek 293/TLR9 cells with CpG oligodeoxynucleotide (ODN). In agreement with previous reports (22), overexpression of full-length IRF5 transactivated the *TNFA* promoter reporter, and this was further elevated in response to CpG ODN (Fig. 8B). Similar to data from the ISRE reporter, the
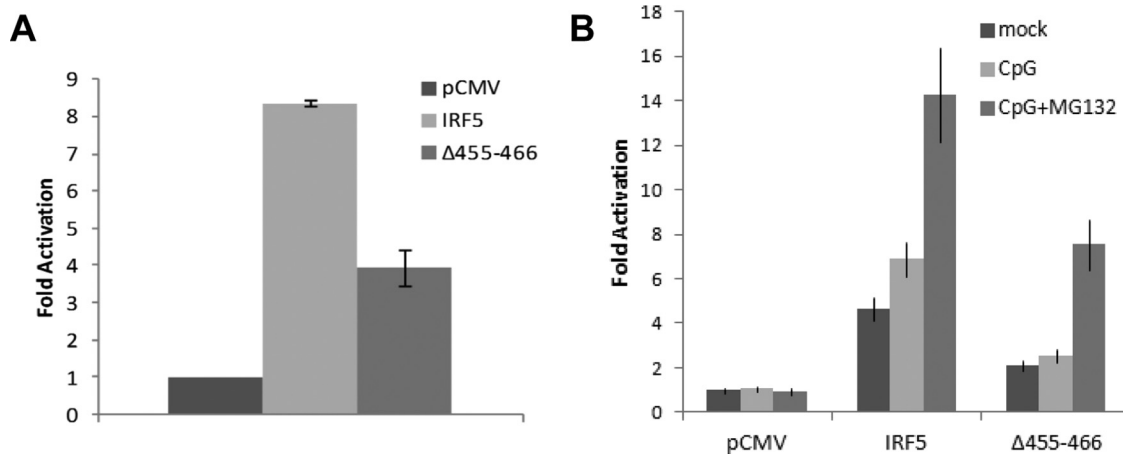
FIG 8 Loss of the CSN/IRF5 interaction diminishes IRF5 transactivation ability. (A) Plasmids encoding Flag-tagged IRF5, the Δ455-466 mutant, and empty vector control (pCMV) were cotransfected with the 5×*ISRE* luciferase promoter reporter, and promoter transactivation was determined by the dual-luciferase assay. Independent experiments were repeated in duplicate wells at least three times; means ± SD are plotted. (B) Same as that described for panel A except that transactivation of the *TNFA* promoter reporter was determined in Hek 293/TLR9 cells left unstimulated (mock) or stimulated with CpG ODN (CpG) or the combination of CpG and MG132. Three independent experiments were repeated in duplicate; means ± SD are plotted.

Δ455-466 IRF5 mutant was ineffective in its transactivation of the *TNFA* promoter either alone or in response to CpG stimulation. To confirm that a loss in IRF5 protein stability diminishes its transactivation potential, IRF5-transfected and CpG-stimulated cells were treated with MG132. We found that the transactivation ability of both full-length and mutant IRF5 was enhanced by the inhibition of proteasome degradation, albeit to different extents (Fig. 8B). The combined treatment of Δ455-466 IRF5-expressing cells with CpG and MG132 gave levels of transactivation similar to that of full-length IRF5 stimulated with CpG; the transactivation ability of CpG-induced full-length IRF5 was greatly enhanced by MG132. Together, these data provide clear evidence that disruption of the CSN/IRF5 interaction decreases IRF5 transactivation ability while inhibition of IRF5 degradation by the proteasome enhances it.

DISCUSSION

The ability of diverse transcription factors to create multiprotein complexes having various biological activities is a trademark of eukaryotic gene regulation. Indeed, protein-protein interactions depict central roles in the activity of IRFs, and diverse protein complexes have been reported (60–63). In the current study, we identified the COP9 signalosome as a new interacting partner of IRF5 that controls its stability through a mechanism involving the ubiquitin-proteasome pathway. This is a novel finding that provides significant new insight into an aspect of IRF5 function about which little is known—the mechanism(s) regulating IRF5 protein stability. Interestingly, another IRF family member, IRF8 (ICSBP), has been shown to interact directly with CSN2 (64). Although the findings of Cohen et al. are distinct from ours, these authors reported that the CSN2/IRF8 interaction resulted in IRF8 phosphorylation that was essential for interaction with IRF1 and thus downstream regulation of its transcriptional activities (64). The CSN-associated kinase(s) responsible for IRF8 phosphorylation is not known. This brings up an interesting possibility for IRF5: can the CSN/IRF5 interaction be used to identify the critical kinase(s) responsible for IRF5 activation? This is a topic that has proven elusive to many of us in the field of IRF research. Nonetheless, these data suggest that the CSN complex may have a central role in regulating the stability, activation, and function of other IRF family members. Indeed, we were able to detect binding of CSN subunits to endogenous IRF7 as well (J. Korczeniewska and B. J. Barnes, unpublished data).

When the CSN was first purified from mammalian cells, it copurified with a Ser/Thr kinase activity against several important signaling molecules, including IκB, p105 (24,

45), and c-Jun (46). Subsequent studies revealed that p53 (44), NF-κB (65, 66), p27^{kip1} (56), and IRF8 (64) were phosphorylated by CSN-associated kinases. The first identified CSN-associated kinase was inositol 1,3,4-triphosphate 5/6 kinase (45, 46), and later, casein kinase 2 (CK2) (42, 44), protein kinase D (PKD) (42), and Akt (50) were identified. The CSN-associated protein kinase(s) phosphorylates transcription factors and controls their stability toward the ubiquitin-proteasome pathway (24, 42, 44, 67). This has been shown for p53, where CSN-dependent phosphorylation of p53 results in degradation (44). The CSN complex has been viewed as a scaffold for spatial sequestration of multiple interacting molecules that exists during the entire protein life cycle and serves as a pivotal regulatory locus for signal transduction (68, 69).

Throughout the literature, there have been many examples revealing the involvement of the CSN complex in important biological functions, such as cell cycle regulation (56, 70–73), signal transduction (53, 55, 65, 74), checkpoint control (51, 54, 57, 75–78), apoptosis (79, 80), and autophagy (81). The CSN is a multifunctional protein complex involved in these different biological responses through its ability to regulate protein stability, transcription, protein phosphorylation, and intracellular distribution (68). All of these functional aspects of the CSN are elements known to be important for IRF5 activation and function. To gain more insight into the functional consequence(s) of the CSN/IRF5 interaction, we used an endogenous model of TRAIL-induced IRF5 activation. We found that activation, i.e., phosphorylation (12), of IRF5 in response to TRAIL treatment resulted in enhanced degradation due to loss of the CSN/IRF5 interaction (Fig. 7). These data suggest that stimuli inducing IRF5 phosphorylation may trigger its subsequent degradation; however, previous work in the laboratory has shown that different stimuli induce different types of IRF5 phosphorylation (13, 19), and therefore some stimuli may work by disrupting the CSN/IRF5 interaction while others may stabilize it. The physiological significance of this interaction was further explored by examining whether loss of the CSN/IRF5 interaction or inhibition of IRF5 proteasome degradation by MG132 altered IRF5 transactivation ability. Indeed, we found that the Δ455-466 mutant was less functional in promoter reporter assays even after stimulation with the TLR9 ligand CpG. Importantly, stabilization of full-length and mutant IRF5 proteins by treatment of cells with MG132 further enhanced IRF5 transactivation potential, supporting the idea that stabilization of the CSN/IRF5 interaction may enhance IRF5 transactivation ability, as seen in mock-treated cells (Fig. 8B).

Based on these data, we propose a general model for IRF5 stabilization and activation (Fig. 9). In unstimulated cells, cytoplasmic IRF5 monomers constitutively interact with CSN subunits at both the carboxyl- and amino-terminal regions, thus stabilizing the masking of the DNA binding domain of IRF5 by the AID (Fig. 9A). This, in turn, leads to effective blocking of IRF5 transcriptional activity and protection from degradation by the ubiquitin-proteasome pathway. IRF5 is in an inactive yet stable conformation ready for activation by an extracellular stressor/stimulus (Fig. 9A). Upon stimulation with TRAIL (or other activation triggers), an as yet to be identified kinase(s) uses the CSN complex as a scaffold and phosphorylates IRF5 and/or CSN subunits that in turn phosphorylate IRF5 (Fig. 9B). The phosphorylation of IRF5 causes a structural change that leads to dissociation from the CSN complex (Fig. 9C). The loss of the CSN/IRF5 interaction then results in K48-linked ubiquitination of IRF5 and degradation by the ubiquitin-proteasome pathway (Fig. 9D), while the remaining "protected" IRF5 is simultaneously in an active state ready for translocation to the nucleus and transactivation of target genes (Fig. 9E). In this model, a tight control exists between the activation and degradation of IRF5, which is expected to allow for a very fine-tuned regulation of IRF5 expression, activation, and target gene expression. This model is supported by our previous work (19) and more recent findings from the crystal structure of IRF5 (48). Together, these data indicate that phosphorylation activates IRF5 by triggering a conformational rearrangement(s) that results in dissociation from the CSN, release of the C-terminal AID segment from autoinhibitory masking of the DNA binding domain to a facilitator of dimerization, and cessation of IRF5-mediated signal-
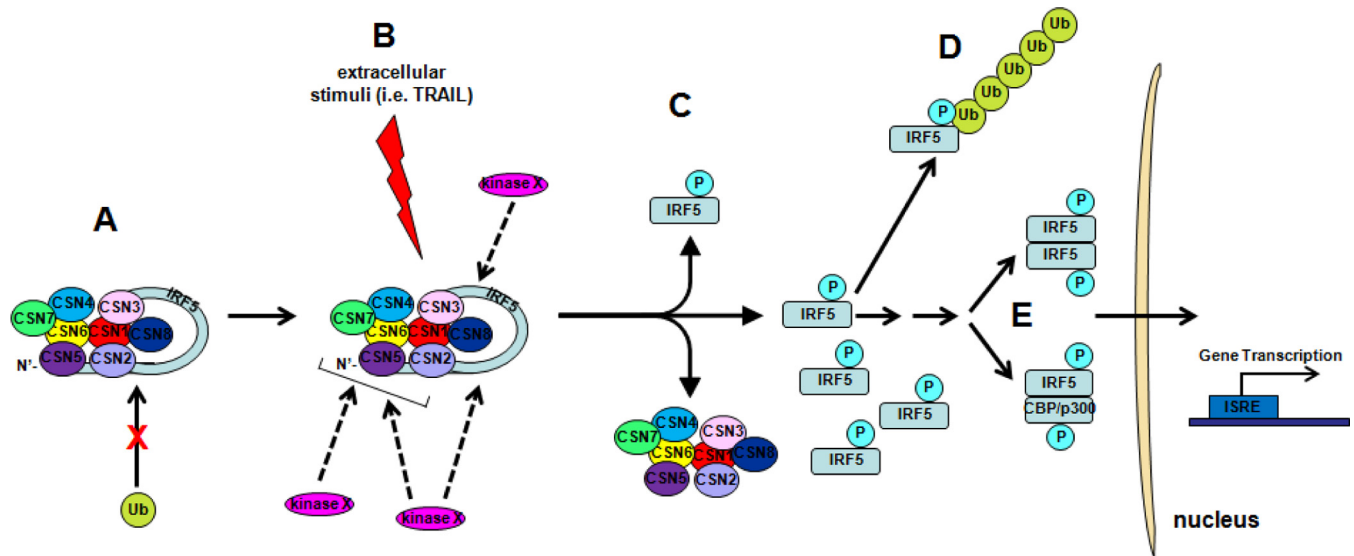
FIG 9 Model of IRF5 stabilization and activation. (A) In unstimulated cells, cytoplasmic IRF5 monomers constitutively interact with CSN subunits at both the carboxyl- and amino-terminal regions, thus masking the DNA binding domain of IRF5 by the AID. This leads to the effective blocking of IRF5 transcriptional activity in unstimulated cells and protects IRF5 from degradation by the ubiquitin-proteasome pathway. (B) Upon stimulation with an activation trigger such as TRAIL, an as yet to be identified kinase(s) (kinase x) uses the CSN complex as a scaffold and phosphorylates IRF5 and/or CSN subunits that in turn phosphorylate IRF5. (C) Phosphorylation of IRF5 results in structural changes that lead to dissociation from the CSN complex. (D) Loss of the CSN/IRF5 interaction results in K48-linked ubiquitination of IRF5 and degradation by the ubiquitin-proteasome pathway. (E) Some "activated" IRF5 forms homodimers or heterodimers with other proteins, such as CBP/p300, and translocates to the nucleus, where it binds to promoters of target genes and regulates their transcription.

ing through its degradation by the ubiquitin-proteasome pathway. Determining the exact kinetics of IRF5 activation, transcriptional regulation of target genes, and degradation will require further investigation.

Recent support has indicated that IRF5 can be ubiquitinated via K63 linkage in response to TLR signaling and overexpression of MyD88, TRAF6, or RIP2 (18, 20); however, current data are controversial with regard to the exact functional consequence of this ubiquitination and whether it alters IRF5 cellular localization and/or transactivation function. Our data indicate that in the absence of stimulation or interaction with the CSN complex, IRF5 undergoes K48-linked polyubiquitination that targets the protein for degradation. It will be important in the near future to further clarify the types of ubiquitin linkage on IRF5, as well as the kinetics of ubiquitination and phosphorylation, in order to determine exactly how the CSN contributes to these two posttranslational events.

Given that IRF5 has been proposed to play a pathogenic role in both SLE and cancer, it may be relevant to look at alterations in the CSN/IRF5 complex in these two disease settings, since IRF5 expression is significantly upregulated in immune cells of SLE patients and downregulated in many tumor cell types (2, 5, 10, 14, 15). CSN levels have indeed been shown to be significantly altered in different diseases, and deregulation of CSN function causes cancer (82, 83). A CSN5-dependent pathway has recently been identified that links anti-inflammatory and antioxidant gene expression to the TLR pathway in myeloid cells (84). A clearer understanding of exactly how the CSN complex regulates IRF5 stability, as well as its involvement in IRF5 activation, may lead to new avenues for targeting this transcription factor in a disease setting. Data presented herein support that the CSN binding sites on IRF5 could be used as targets for the generation of small-molecule inhibitors. Such inhibitors could theoretically attenuate the levels of IRF5 in a cell and thus may be useful in the treatment of autoimmune diseases such as SLE, where aberrant IRF5 expression and activation have been detected (5, 59).

MATERIALS AND METHODS

Expression plasmids. The pCMV-Tag2.IRF5 and pEGFP.IRF5 mammalian expression plasmids were described previously (2, 19). cDNA of full-length IRF5 variant 4 (residues 1 to 489) was used to create amino- and carboxyl-terminal deletions, truncated to the amino acids indicated in Fig. 2A. Mutants were constructed by PCR amplification of the full-length IRF5 template with *Pfu* Turbo DNA polymerase (Stratagene) and subcloned into EcoRI-SalI sites of plasmid pCMVTag2B (Stratagene) as previously described (19). Internal deletion mutants at the amino- and carboxyl-terminal ends were generated using the QuikChange II site-directed mutagenesis kit (Promega). Sequences of the PCR-generated portion of all constructs were verified by DNA sequencing and confirmed to express protein by Western blotting with anti-Flag M2 antibodies (Sigma-Aldrich) or anti-IRF5 antibodies (Cell Signaling). The CSN2 expression plasmid was a kind gift from B. Z. Levi (Technion, Haifa, Israel), CSN3 was from W. Dubiel (Charite University, Berlin, Germany), and CSN5 was from M. Neumann (Otto-von-Guericke University, Magde-burg, Germany). The HA-Ub plasmid was a kind gift from I. P. Whitehead (UMDNJ), and the *TNFA* promoter reporter was from A. Goldfeld (Harvard Medical School).

Cell culture. Hek 293T cells were a generous gift from I. P. Whitehead (UMDNJ, Newark, NJ) and were maintained at 37°C (5% CO_2) in Dulbecco's modified Eagle's medium (DMEM; high glucose) supplemented with 10% fetal bovine serum (FBS) (Sigma) and 2 mM glutamine without antibiotics. Hek 293 cells stably expressing TLR9 were purchased from InvivoGen and maintained in a similar manner. THP-1 cells were kindly provided by M. B. Mathews (UMDNJ, Newark, NJ) and were grown at 37°C (5% CO_2) in RPMI 1640 supplemented with 10% FBS and 2 mM L-glutamine (Gemini Bio-Products) without antibiotics.

Transient transfections, siRNA knockdown, and cycloheximide chase. Hek 293T cells at 40% confluence were transfected with IRF5 expression plasmids (2 μg/6-well plate, 4 μg/60-mm-diameter plate, 8 μg/100-mm-diameter plate) using Lipofectamine 2000 reagent (Invitrogen) in accordance with the manufacturer's instructions. The DNA transient transfections were carried out for 32 h unless otherwise indicated. A modified protocol from Bi et al. (15) was used to transfect siRNAs into Hek 293T and THP-1 cells. Hek 293T cells were transiently transfected with 20 pmol of each siRNA, i.e., siGenome lamin A/C control siRNA (Dharmacon), CSN1 siRNA, or CSN3 siRNA, or were cotransfected simultaneously with CSN1 and CSN3 siRNAs (Santa Cruz Biotechnology) using Lipofectamine 2000. Twenty-four hours following transfection, the cells were transfected two more times at the 24-h time points with an additional 20 pmol of each siRNA. Similarly, 3×10^6 THP-1 cells were transfected twice (a second time at the 24-h time point) with 20 pmol of siRNAs using Hypoosmolar electroporation buffer (Eppendorf) and the Gene Pulser Xcell electroporation system (Bio-Rad). All siRNA transfections were carried out for 72 h, and knockdown efficiency was determined by Western blotting. For protein stability assays, Hek 293T cells were fed after transfection with fresh medium and treated with 100 μg/ml cycloheximide (CHX) (Sigma-Aldrich), CHX and 50 μM ubiquitin-activating enzyme inhibitor (UBEI-41) (BioGenova), or CHX and 25 μM proteasome inhibitor (MG-132) (EMD Chemicals) for the time periods indicated in Fig. 6A. Similarly, untransfected THP-1 cells were treated with 100 μg/ml CHX and/or 25 ng/ml Superkiller TRAIL (Alexis Biochemicals) for the indicated time periods.

Immunoprecipitation and Western blot analysis. Cells were harvested using lysis buffer (50 mM Tris-HCl, pH 7.4, 2 mM $MgCl_2$, 100 mM NaCl, 10% glycerol, 1% Nonidet P-40 [Sigma-Aldrich]) supplemented with 0.2 mM protease inhibitor cocktail (Sigma-Aldrich). Protein extracts (300 μg) from transfected cells were precipitated with anti-Flag M2 affinity gel antibodies (Sigma-Aldrich) by rotation at 4°C for 2 h, and immunoprecipitates were washed three times with ice-cold lysis buffer. Proteins were eluted by boiling the beads for 5 min in 2× SDS loading dye, separated by 10% SDS-PAGE, transferred to a nitrocellulose membrane, and blocked for 1 h at room temperature with 5% nonfat milk in Tris-buffered saline–Tween 20 (TBST). Membranes were then incubated with anti-human CSN1 at a 1:3,000 dilution, CSN2 (1:10,000), CSN4 (1:1,000), CSN5 (1:2,000), CSN6 (1:1,000), CSN7 (1:5,000), and CSN8 (1:5,000) rabbit polyclonal antibodies (PAb) (Enzo Life Sciences); anti-human CSN3 rabbit monoclonal antibodies (MAb) (Epitomics) and M2 anti-Flag mouse monoclonal antibodies (Sigma-Aldrich) were used at a 1:10,000 dilution. Anti-human IRF5 rabbit PAb, anti-β-actin (13E5) rabbit MAb (horseradish peroxidase [HRP] conjugate), anti-GAPDH (14C10) rabbit MAb (HRP conjugate), anti-K48-linkage-specific polyubiquitination (D9D5) rabbit MAb, and antiubiquitin (P4D1) mouse MAb (all from Cell Signaling) were used at a 1:1,000 dilution. Secondary HRP-conjugated anti-mouse or anti-rabbit immunoglobulin G antibodies (Cell Signaling) were used at 1:2,000 dilutions, and proteins were visualized with enhanced chemiluminescence (ECL) detection reagent (GE Healthcare), followed by autoradiography using HyBlot CL film (Denville Scientific). Immunoprecipitation of endogenous proteins (400 μg) was performed in a similar manner with anti-human IRF5 PAb and normal rabbit IgG antibodies.

Dual-luciferase assay. Hek 293T or Hek 293/TLR9-expressing cells were transiently transfected using Lipofectamine 2000 (Invitrogen). A 1:1 ratio (2 μg each) of luciferase reporter and IRF5 expression plasmid along with 0.1 μg of pRL-CMV as an internal control was used. Cells were left untreated or were treated with CpG ODN 2216 (Invivogen) and MG132, where indicated, harvested 24 h posttransfection, and lysed with passive lysis buffer (Promega). Luciferase assays were carried out using the Dual-Luciferase assay kit according to the manufacturer's specifications (Promega). The levels of reporter firefly luciferase activity were normalized to a constant level of pRL-CMV activity; values were normalized to the luciferase readings from an empty vector control.

Flow cytometry. Hek 293T cells were transiently transfected with pEGFPC2.IRF5 or pEGFPC2.Δ455-466 plasmid as described above. At 48 h posttransfection, cells were collected by trypsinization, washed, and resuspended in DMEM with 20% FBS. Cells were sorted on a BD FACSAria II SORP into subpopulations expressing low, medium, and high levels of GFP, as described previously (49). Cells expressing medium levels of GFP-IRF5 were replated and treated with 100 μg/ml CHX for 30 to 300 min and then

collected and fixed in 1% formaldehyde at 4°C. Cells expressing GFP-IRF5 were gated on and IRF5 expression was examined using a FACSCalibur flow cytometer (BD Biosciences). GFP levels were analyzed using CellQuest software (BD Biosciences). To compare the relative stabilities of full-length IRF5 and the Δ455-466 mutant, a linear regression analysis of mean fluorescence as a function of time was performed. A similar analysis was performed independently on transiently transfected cells without sorting first for cells that express medium levels of GFP-IRF5.

Amnis Imagestream. THP-1 cells were treated with 25 ng/ml Superkiller TRAIL (Alexis Biochemicals) for the indicated time periods. Cells were permeabilized with 0.1% Triton X-100 (Fisher Scientific) and intracellularly stained with polyclonal anti-IRF5 antibody (32.5 ng/μl; Cell Signaling, Danvers, MA), followed by FITC-conjugated anti-rabbit secondary antibody (10 ng/μl; BD Pharmingen, San Jose, CA); nuclei were stained with DRAQ5 (10 μM) immediately before acquisition. Samples were acquired using an ImageStream 100 flow cytometer and analyzed with IDEAS software (Amnis Corporation, Seattle, WA) as recently described (59). In brief, single focused cells were identified by gating on DRAQ5-positive events with high DRAQ5 aspect ratios (minor axis divided by major axis, measure of single event) and high nuclear contrast (measured by the Gradient RMS feature). Nuclear localization of IRF5 was measured using a morphology mask to determine a similarity score, which quantifies the correlation of pixel values of the DRAQ5 and IRF5 images on a per-cell basis. A similarity score of >1 was used as a cutoff for nuclear-localized IRF5; cells in individual bins were visually inspected to confirm subcellular localization (values of <1 or >1). IDEAS software then generates a composite view of single and merged stains from all acquired cells.

2-D gel electrophoresis and protein quantification. 2-D gel electrophoresis was performed as previously described (85). Proteins bound to M2 anti-Flag beads were eluted by incubating the beads in 185 μl of isoelectric focusing rehydration buffer (7 M urea, 2 M thiourea, 4% CHAPS {3-[(3-cholamidopropyl)-dimethylammonio]-1-propanesulfonate}, 100 mM dithiothreitol [DTT], 0.2% biolytes [pH 5 to 8], 0.01% bromophenol blue, and protease inhibitor). Eluted proteins in a total of 185 μl of the rehydration buffer were applied to 11-cm Bio-Rad ReadyStrip IPG strips (pH 5 to 8) for overnight rehydration. First-dimension isoelectric focusing was performed on a Bio-Rad (Hercules, CA) Protean isoelectric focusing system at the University of Medicine and Dentistry of New Jersey Center for Advanced Proteomics Research (http://njms.rutgers.edu/proweb/), as described by the manufacturer, for a total focusing time of 75,000 V/h. Strips were equilibrated with equilibration solution I (6 M urea, 0.375 M Tris-HCl, pH 8.8, 2% SDS, 20% glycerol, 2% [wt/vol] DTT) for 15 min and then with equilibration solution II (6 M urea, 0.375 M Tris-HCl, pH 8.8, 2% SDS, 20% glycerol, 2.5% [wt/vol] iodoacetamide) for 15 min and directly applied to a 12.5% isocratic SDS-polyacrylamide gel for the second-dimension electrophoresis. The gel was fixed in a solution consisting of 10% acetic acid and 40% ethanol for 30 min and stained overnight with SYPRO ruby (Molecular Probes, OR). Gels were destained with a solution containing 10% methanol and 7.5% acetic acid for 2 h at room temperature and scanned on a Typhoon 9400 variable-mode imager (GE Healthcare, Piscataway, NJ) using a green laser (532 nm) and a 610BP30 emission filter. Protein quantitation on SYPRO ruby-stained gels was performed by PDQuest 2-D analysis software (Bio-Rad), and protein spots whose expression levels appreciably changed between the control and experiment were isolated for mass spectrometric identification.

MS and protein identification. Protein bands/spots from SYPRO ruby-stained gels were isolated for protein identification. Gel bands were diced into 1-mm³ pieces and washed with 30% acetonitrile (ACN) in 50 mM ammonium bicarbonate before DTT reduction and iodoacetamide alkylation. Trypsin was used for digestion at 37°C overnight. The resulting peptides were extracted with 30 μl of 1% trifluoroacetic acid, followed by C$_{18}$ ZipTip desalting. For the mass spectrometry (MS) analysis, peptides were mixed with 7 mg/ml α-cyano-4-hydroxy-cinnamic acid matrix (in 60% ACN) at a 1:1 ratio and spotted onto a matrix-assisted laser desorption ionization (MALDI) plate; peptides were analyzed on a 4800 MALDI-TOF/TOF mass analyzer (Applied Biosystems, Framingham, MA). Mass spectra (m/z 880 to 3,200) were acquired in the positive ion reflector mode. The 15 most intense ions were selected for the subsequent MS-MS sequencing analysis in a 1-kV mode. Protein identification was performed by searching the combined tandem mass spectra against the NCBI (National Center for Biotechnology Information) human sequence database using a local MASCOT search engine (v.1.9) on a GPS (v.3.5; ABI) server. Proteins containing at least one peptide with a confidence interval of ≥95% were considered to have been positively identified.

Preparation of recombinant proteins. Recombinant IRF5, CSN2, CSN3, and CSN5 were generated by *in vitro* transcription/translation via the relevant expression plasmids and the TNT coupled reticulocyte lysate system (Promega) according to the manufacturer's specifications. Briefly, by use of the Transcend nonradioactive translation detection system (Promega), biotinylated lysine residues were incorporated into nascent IRF5 protein during translation. At the same time, MagneSphere paramagnetic particles (SA-PMPs) (Promega) were washed three times in 1 ml of PBS, captured using a magnetic stand, and resuspended in 60 μl phosphate-buffered saline (PBS). Biotinylated protein-protein complexes (50 μl) were added to the beads and incubated by rotation at room temperature for 30 min. Following the binding reaction, bead-protein complexes were washed three times with 1 ml of PBS and captured with the magnetic stand; bound proteins were eluted by boiling in 2× SDS loading dye and resolving on a 10% SDS-PAGE gel. Membranes were immunoblotted with the indicated antibodies.

Statistical analysis. Statistical analysis was done with the two-tailed Student *t* test or Mann-Whitney *U* test when variables were not normally distributed. Data are presented as the mean ± standard deviation (SD) (normal distribution) or the mean ± standard error of the mean (SEM) (nonnormal

distribution). A P value of <0.05 was considered significant. Statistical analyses were performed using Prism 4.0 (GraphPad Software, San Diego, CA).

ACKNOWLEDGMENTS

REFERENCES

1. Savitsky D, Tamura T, Yanai H, Taniguchi T. 2010. Regulation of immunity and oncogenesis by the IRF transcription factor family. Cancer Immunol Immunother 59:489–510. https://doi.org/10.1007/s00262-009-0804-6.

2. Barnes BJ, Moore PA, Pitha PM. 2001. Virus-specific activation of a novel interferon regulatory factor, IRF-5, results in the induction of distinct interferon alpha genes. J Biol Chem 276:23382–23390. https://doi.org/10.1074/jbc.M101216200.

3. Takaoka A, Yanai H, Kondo S, Duncan G, Negishi H, Mizutani T, Kano S, Honda K, Ohba Y, Mak TW, Taniguchi T. 2005. Integral role of IRF-5 in the gene induction programme activated by Toll-like receptors. Nature 434: 243–249. https://doi.org/10.1038/nature03308.

4. Yanai H, Chen HM, Inuzuka T, Kondo S, Mak TW, Takaoka A, Honda K, Taniguchi T. 2007. Role of IFN regulatory factor 5 transcription factor in antiviral immunity and tumor suppression. Proc Natl Acad Sci U S A 104:3402–3407. https://doi.org/10.1073/pnas.0611559104.

5. Feng D, Stone RC, Eloranta ML, Sangster-Guity N, Nordmark G, Sigurdsson S, Wang C, Alm G, Syvanen AC, Ronnblom L, Barnes BJ. 2010. Genetic variants and disease-associated factors contribute to enhanced interferon regulatory factor 5 expression in blood cells of patients with systemic lupus erythematosus. Arthritis Rheum 62:562–573.

6. Miceli-Richard C, Comets E, Loiseau P, Puechal X, Hachulla E, Mariette X. 2007. Association of an IRF5 gene functional polymorphism with Sjogren's syndrome. Arthritis Rheum 56:3989–3994. https://doi.org/10.1002/art.23142.

7. Rueda B, Reddy MV, Gonzalez-Gay MA, Balsa A, Pascual-Salcedo D, Petersson IF, Eimon A, Paira S, Scherbarth HR, Pons-Estel BA, Gonzalez-Escribano MF, Alarcon-Riquelme ME, Martin J. 2006. Analysis of IRF5 gene functional polymorphisms in rheumatoid arthritis. Arthritis Rheum 54:3815–3819. https://doi.org/10.1002/art.22271.

8. Sigurdsson S, Nordmark G, Goring HH, Lindroos K, Wiman AC, Sturfelt G, Jonsen A, Rantapaa-Dahlqvist S, Moller B, Kere J, Koskenmies S, Widen E, Eloranta ML, Julkunen H, Kristjansdottir H, Steinsson K, Alm G, Ronnblom L, Syvanen AC. 2005. Polymorphisms in the tyrosine kinase 2 and interferon regulatory factor 5 genes are associated with systemic lupus erythematosus. Am J Hum Genet 76:528–537. https://doi.org/10.1086/428480.

9. Sigurdsson S, Padyukov L, Kurreeman FA, Liljedahl U, Wiman AC, Alfredsson L, Toes R, Ronnelid J, Klareskog L, Huizinga TW, Alm G, Syvanen AC, Ronnblom L. 2007. Association of a haplotype in the promoter region of the interferon regulatory factor 5 gene with rheumatoid arthritis. Arthritis Rheum 56:2202–2210. https://doi.org/10.1002/art.22704.

10. Barnes BJ, Kellum MJ, Pinder KE, Frisancho JA, Pitha PM. 2003. Interferon regulatory factor 5, a novel mediator of cell cycle arrest and cell death. Cancer Res 63:6424–6431.

11. Couzinet A, Tamura K, Chen HM, Nishimura K, Wang Z, Morishita Y, Takeda K, Yagita H, Yanai H, Taniguchi T, Tamura T. 2008. A cell-type-specific requirement for IFN regulatory factor 5 (IRF5) in Fas-induced apoptosis. Proc Natl Acad Sci U S A 105:2556–2561. https://doi.org/10.1073/pnas.0712295105.

12. Hu G, Barnes BJ. 2009. IRF-5 is a mediator of the death receptor-induced apoptotic signaling pathway. J Biol Chem 284:2767–2777. https://doi.org/10.1074/jbc.M804744200.

13. Hu G, Mancl ME, Barnes BJ. 2005. Signaling through IFN regulatory factor-5 sensitizes p53-deficient tumors to DNA damage-induced apoptosis and cell death. Cancer Res 65:7403–7412. https://doi.org/10.1158/0008-5472.CAN-05-0583.

14. Mori T, Anazawa Y, Iiizumi M, Fukuda S, Nakamura Y, Arakawa H. 2002. Identification of the interferon regulatory factor 5 gene (IRF-5) as a direct target for p53. Oncogene 21:2914–2918. https://doi.org/10.1038/sj.onc.1205459.

15. Bi X, Hameed M, Mirani N, Pimenta EM, Anari J, Barnes BJ. 2011. Loss of interferon regulatory factor 5 (IRF5) expression in human ductal carcinoma correlates with disease stage and contributes to metastasis. Breast Cancer Res 13:R111. https://doi.org/10.1186/bcr3053.

16. Izaguirre A, Barnes BJ, Amrute S, Yeow WS, Megjugorac N, Dai J, Feng D, Chung E, Pitha PM, Fitzgerald-Bocarsly P. 2003. Comparative analysis of IRF and IFN-alpha expression in human plasmacytoid and monocyte-derived dendritic cells. J Leukoc Biol 74:1125–1138. https://doi.org/10.1189/jlb.0603255.

17. Mancl ME, Hu G, Sangster-Guity N, Olshalsky SL, Hoops K, Fitzgerald-Bocarsly P, Pitha PM, Pinder K, Barnes BJ. 2005. Two discrete promoters regulate the alternatively spliced human interferon regulatory factor-5 isoforms. Multiple isoforms with distinct cell type-specific expression, localization, regulation, and function. J Biol Chem 280:21078–21090.

18. Balkhi MY, Fitzgerald KA, Pitha PM. 2008. Functional regulation of MyD88-activated interferon regulatory factor 5 by K63-linked polyubiquitination. Mol Cell Biol 28:7296–7308. https://doi.org/10.1128/MCB.00662-08.

19. Barnes BJ, Kellum MJ, Field AE, Pitha PM. 2002. Multiple regulatory domains of IRF-5 control activation, cellular localization, and induction of chemokines that mediate recruitment of T lymphocytes. Mol Cell Biol 22:5721–5740. https://doi.org/10.1128/MCB.22.16.5721-5740.2002.

20. Chang Foreman HC, Van Scoy S, Cheng TF, Reich NC. 2012. Activation of interferon regulatory factor 5 by site specific phosphorylation. PLoS One 7:e33098. https://doi.org/10.1371/journal.pone.0033098.

21. Cheng TF, Brzostek S, Ando O, Van Scoy S, Kumar KP, Reich NC. 2006. Differential activation of IFN regulatory factor (IRF)-3 and IRF-5 transcription factors during viral infection. J Immunol 176:7462–7470. https://doi.org/10.4049/jimmunol.176.12.7462.

22. Feng D, Sangster-Guity N, Stone R, Korczeniewska J, Mancl ME, Fitzgerald-Bocarsly P, Barnes BJ. 2010. Differential requirement of histone acetylase and deacetylase activities for IRF5-mediated proinflammatory cytokine expression. J Immunol 185:6003–6012. https://doi.org/10.4049/jimmunol.1000482.

23. Barnes BJ, Field AE, Pitha-Rowe PM. 2003. Virus-induced heterodimer formation between IRF-5 and IRF-7 modulates assembly of the IFNA enhanceosome in vivo and transcriptional activity of IFNA genes. J Biol Chem 278:16630–16641. https://doi.org/10.1074/jbc.M212609200.

24. Seeger M, Kraft R, Ferrell K, Bech-Otschir D, Dumdey R, Schade R, Gordon C, Naumann M, Dubiel W. 1998. A novel protein complex involved in signal transduction possessing similarities to 26S proteasome subunits. FASEB J 12:469–478.

25. Wei N, Tsuge T, Serino G, Dohmae N, Takio K, Matsui M, Deng XW. 1998. The COP9 complex is conserved between plants and mammals and is related to the 26S proteasome regulatory complex. Curr Biol 8:919–922. https://doi.org/10.1016/S0960-9822(07)00372-7.

26. Chamovitz DA, Wei N, Osterlund MT, von Arnim AG, Staub JM, Matsui M, Deng XW. 1996. The COP9 complex, a novel multisubunit nuclear regulator involved in light control of a plant developmental switch. Cell 86:115–121. https://doi.org/10.1016/S0092-8674(00)80082-3.

27. Wei N, Chamovitz DA, Deng XW. 1994. Arabidopsis COP9 is a component of a novel signaling complex mediating light control of development. Cell 78:117–124. https://doi.org/10.1016/0092-8674(94)90578-9.

28. Wei N, Deng XW. 1999. Making sense of the COP9 signalosome. A regulatory protein complex conserved from Arabidopsis to human. Trends Genet 15:98–103.

29. Mundt KE, Porte J, Murray JM, Brikos C, Christensen PU, Caspari T, Hagan IM, Millar JB, Simanis V, Hofmann K, Carr AM. 1999. The COP9/signalosome complex is conserved in fission yeast and has a role in S phase. Curr Biol 9:1427–1430. https://doi.org/10.1016/S0960-9822(00)80091-3.

30. Busch S, Eckert SE, Krappmann S, Braus GH. 2003. The COP9 signalosome is an essential regulator of development in the filamentous fungus Aspergillus nidulans. Mol Microbiol 49:717–730. https://doi.org/10.1046/j.1365-2958.2003.03612.x.

31. Luke-Glaser S, Roy M, Larsen B, Le Bihan T, Metalnikov P, Tyers M, Peter M, Pintard L. 2007. CIF-1, a shared subunit of the COP9/signalosome and eukaryotic initiation factor 3 complexes, regulates MEL-26 levels in the Caenorhabditis elegans embryo. Mol Cell Biol 27:4526–4540. https://doi.org/10.1128/MCB.01724-06.

32. Bech-Otschir D, Seeger M, Dubiel W. 2002. The COP9 signalosome: at the interface between signal transduction and ubiquitin-dependent proteolysis. J Cell Sci 115:467–473.

33. Cope GA, Deshaies RJ. 2003. COP9 signalosome: a multifunctional regulator of SCF and other cullin-based ubiquitin ligases. Cell 114:663–671. https://doi.org/10.1016/S0092-8674(03)00722-0.

34. Schwechheimer C. 2004. The COP9 signalosome (CSN): an evolutionary conserved proteolysis regulator in eukaryotic development. Biochim Biophys Acta 1695:45–54. https://doi.org/10.1016/j.bbamcr.2004.09.023.

35. von Arnim AG. 2003. On again-off again: COP9 signalosome turns the key on protein degradation. Curr Opin Plant Biol 6:520–529. https://doi.org/10.1016/j.pbi.2003.09.006.

36. Wei N, Deng XW. 2003. The COP9 signalosome. Annu Rev Cell Dev Biol 19:261–286. https://doi.org/10.1146/annurev.cellbio.19.111301.112449.

37. Wolf DA, Zhou C, Wee S. 2003. The COP9 signalosome: an assembly and maintenance platform for cullin ubiquitin ligases? Nat Cell Biol 5:1029–1033. https://doi.org/10.1038/ncb1203-1029.

38. Harari-Steinberg O, Chamovitz DA. 2004. The COP9 signalosome: mediating between kinase signaling and protein degradation. Curr Protein Pept Sci 5:185–189. https://doi.org/10.2174/1389203043379792.

39. Kim JH, Choi JK, Cinghu S, Jang JW, Lee YS, Li YH, Goh YM, Chi XZ, Lee KS, Wee H, Bae SC. 2009. Jab1/CSN5 induces the cytoplasmic localization and degradation of RUNX3. J Cell Biochem 107:557–565. https://doi.org/10.1002/jcb.22157.

40. Oh W, Lee EW, Sung YH, Yang MR, Ghim J, Lee HW, Song J. 2006. Jab1 induces the cytoplasmic localization and degradation of p53 in coordination with Hdm2. J Biol Chem 281:17457–17465. https://doi.org/10.1074/jbc.M601857200.

41. Hoareau Alves K, Bochard V, Rety S, Jalinot P. 2002. Association of the mammalian proto-oncoprotein Int-6 with the three protein complexes eIF3, COP9 signalosome and 26S proteasome. FEBS Lett 527:15–21. https://doi.org/10.1016/S0014-5793(02)03147-2.

42. Uhle S, Medalia O, Waldron R, Dumdey R, Henklein P, Bech-Otschir D, Huang X, Berse M, Sperling J, Schade R, Dubiel W. 2003. Protein kinase CK2 and protein kinase D are associated with the COP9 signalosome. EMBO J 22:1302–1312. https://doi.org/10.1093/emboj/cdg127.

43. Wang Y, Devereux W, Stewart TM, andCasero RA, Jr. 2001. Characterization of the interaction between the transcription factors human polyamine modulated factor (PMF-1) and NF-E2-related factor 2 (Nrf-2) in the transcriptional regulation of the spermidine/spermine N1-acetyltransferase (SSAT) gene. Biochem J 355:45–49. https://doi.org/10.1042/bj3550045.

44. Bech-Otschir D, Kraft R, Huang X, Henklein P, Kapelari B, Pollmann C, Dubiel W. 2001. COP9 signalosome-specific phosphorylation targets p53 to degradation by the ubiquitin system. EMBO J 20:1630–1639. https://doi.org/10.1093/emboj/20.7.1630.

45. Sun Y, Wilson MP, Majerus PW. 2002. Inositol 1,3,4-trisphosphate 5/6-kinase associates with the COP9 signalosome by binding to CSN1. J Biol Chem 277:45759–45764. https://doi.org/10.1074/jbc.M208709200.

46. Wilson MP, Sun Y, Cao L, Majerus PW. 2001. Inositol 1,3,4-trisphosphate 5/6-kinase is a protein kinase that phosphorylates the transcription factors c-Jun and ATF-2. J Biol Chem 276:40998–41004. https://doi.org/10.1074/jbc.M106605200.

47. Tomoda K, Kubota Y, Arata Y, Mori S, Maeda M, Tanaka T, Yoshida M, Yoneda-Kato N, Kato JY. 2002. The cytoplasmic shuttling and subsequent degradation of p27Kip1 mediated by Jab1/CSN5 and the COP9 signalosome complex. J Biol Chem 277:2302–2310. https://doi.org/10.1074/jbc.M104431200.

48. Chen W, Lam SS, Srinath H, Jiang Z, Correia JJ, Schiffer CA, Fitzgerald KA, Lin K, andRoyer WE, Jr. 2008. Insights into interferon regulatory factor activation from the crystal structure of dimeric IRF5. Nat Struct Mol Biol 15:1213–1220. https://doi.org/10.1038/nsmb.1496.

49. Jiang X, Coffino P, Li X. 2004. Development of a method for screening short-lived proteins using green fluorescent protein. Genome Biol 5:R81. https://doi.org/10.1186/gb-2004-5-10-r81.

50. Peth A, Berndt C, Henke W, Dubiel W. 2007. Downregulation of COP9 signalosome subunits differentially affects the CSN complex and target protein stability. BMC Biochem 8:27. https://doi.org/10.1186/1471-2091-8-27.

51. Dornan D, Wertz I, Shimizu H, Arnott D, Frantz GD, Dowd P, O'Rourke K, Koeppen H, Dixit VM. 2004. The ubiquitin ligase COP1 is a critical negative regulator of p53. Nature 429:86–92. https://doi.org/10.1038/nature02514.

52. Hetfeld BK, Bech-Otschir D, Dubiel W. 2005. Purification method of the COP9 signalosome from human erythrocytes. Methods Enzymol 398:481–491. https://doi.org/10.1016/S0076-6879(05)98039-7.

53. Luo J, Emanuele MJ, Li D, Creighton CJ, Schlabach MR, Westbrook TF, Wong KK, Elledge SJ. 2009. A genome-wide RNAi screen identifies multiple synthetic lethal interactions with the Ras oncogene. Cell 137:835–848. https://doi.org/10.1016/j.cell.2009.05.006.

54. Shiloh Y. 2006. The ATM-mediated DNA-damage response: taking shape. Trends Biochem Sci 31:402–410. https://doi.org/10.1016/j.tibs.2006.05.004.

55. Tomoda K, Kato JY, Tatsumi E, Takahashi T, Matsuo Y, Yoneda-Kato N. 2005. The Jab1/COP9 signalosome subcomplex is a downstream mediator of Bcr-Abl kinase activity and facilitates cell-cycle progression. Blood 105:775–783. https://doi.org/10.1182/blood-2004-04-1242.

56. Tomoda K, Kubota Y, Kato J. 1999. Degradation of the cyclin-dependent-kinase inhibitor p27Kip1 is instigated by Jab1. Nature 398:160–165. https://doi.org/10.1038/18230.

57. Yoneda-Kato N, Tomoda K, Umehara M, Arata Y, Kato JY. 2005. Myeloid leukemia factor 1 regulates p53 by suppressing COP1 via COP9 signalosome subunit 3. EMBO J 24:1739–1749. https://doi.org/10.1038/sj.emboj.7600656.

58. Schoenemeyer A, Barnes BJ, Mancl ME, Latz E, Goutagny N, Pitha PM, Fitzgerald KA, Golenbock DT. 2005. The interferon regulatory factor, IRF5, is a central mediator of toll-like receptor 7 signaling. J Biol Chem 280:17005–17012. https://doi.org/10.1074/jbc.M412584200.

59. Stone RC, Feng D, Deng J, Singh S, Yang L, Fitzgerald-Bocarsly P, Eloranta ML, Ronnblom L, Barnes BJ. 2012. Interferon regulatory factor 5 activation in monocytes of systemic lupus erythematosus patients is triggered by circulating autoantigens independent of type I interferons. Arthritis Rheum 64:788–798. https://doi.org/10.1002/art.33395.

60. Brass AL, Zhu AQ, Singh H. 1999. Assembly requirements of PU.1-Pip (IRF-4) activator complexes: inhibiting function in vivo using fused dimers. EMBO J 18:977–991. https://doi.org/10.1093/emboj/18.4.977.

61. Eklund EA, Jalava A, Kakar R. 1998. PU.1, interferon regulatory factor 1, and interferon consensus sequence-binding protein cooperate to increase gp91(phox) expression. J Biol Chem 273:13957–13965. https://doi.org/10.1074/jbc.273.22.13957.

62. Kantakamalakul W, Politis AD, Marecki S, Sullivan T, Ozato K, Fenton MJ, Vogel SN. 1999. Regulation of IFN consensus sequence binding protein expression in murine macrophages. J Immunol 162:7417–7425.

63. Sharf R, Azriel A, Lejbkowicz F, Winograd SS, Ehrlich R, Levi BZ. 1995. Functional domain analysis of interferon consensus sequence binding protein (ICSBP) and its association with interferon regulatory factors. J Biol Chem 270:13063–13069. https://doi.org/10.1074/jbc.270.22.13063.

64. Cohen H, Azriel A, Cohen T, Meraro D, Hashmueli S, Bech-Otschir D, Kraft R, Dubiel W, Levi BZ. 2000. Interaction between interferon consensus sequence-binding protein and COP9/signalosome subunit CSN2 (Trip15). A possible link between interferon regulatory factor signaling and the COP9/signalosome. J Biol Chem 275:39081–39089.

65. Schweitzer K, Bozko PM, Dubiel W, Naumann M. 2007. CSN controls NF-kappaB by deubiquitinylation of IkappaBalpha. EMBO J 26:1532–1541. https://doi.org/10.1038/sj.emboj.7601600.

66. Schweitzer K, Naumann M. 2010. Control of NF-kappaB activation by the COP9 signalosome. Biochem Soc Trans 38:156–161. https://doi.org/10.1042/BST0380156.

67. Naumann M, Bech-Otschir D, Huang X, Ferrell K, Dubiel W. 1999. COP9

signalosome-directed c-Jun activation/stabilization is independent of JNK. J Biol Chem 274:35297–35300. https://doi.org/10.1074/jbc.274.50.35297.

68. Kato JY, Yoneda-Kato N. 2009. Mammalian COP9 signalosome. Genes Cells 14:1209–1225. https://doi.org/10.1111/j.1365-2443.2009.01349.x.

69. McCulloch CA, Downey GP, El-Gabalawy H. 2006. Signalling platforms that modulate the inflammatory response: new targets for drug development. Nat Rev Drug Discov 5:864–876. https://doi.org/10.1038/nrd2109.

70. Bondar T, Kalinina A, Khair L, Kopanja D, Nag A, Bagchi S, Raychaudhuri P. 2006. Cul4A and DDB1 associate with Skp2 to target p27Kip1 for proteolysis involving the COP9 signalosome. Mol Cell Biol 26:2531–2539. https://doi.org/10.1128/MCB.26.7.2531-2539.2006.

71. Menon S, Chi H, Zhang H, Deng XW, Flavell RA, Wei N. 2007. COP9 signalosome subunit 8 is essential for peripheral T cell homeostasis and antigen receptor-induced entry into the cell cycle from quiescence. Nat Immunol 8:1236–1245. https://doi.org/10.1038/ni1514.

72. Panattoni M, Sanvito F, Basso V, Doglioni C, Casorati G, Montini E, Bender JR, Mondino A, Pardi R. 2008. Targeted inactivation of the COP9 signalosome impairs multiple stages of T cell development. J Exp Med 205:465–477. https://doi.org/10.1084/jem.20070725.

73. Yang X, Menon S, Lykke-Andersen K, Tsuge T, Di X, Wang X, Rodriguez-Suarez RJ, Zhang H, Wei N. 2002. The COP9 signalosome inhibits p27(kip1) degradation and impedes G1-S phase progression via deneddylation of SCF Cul1. Curr Biol 12:667–672. https://doi.org/10.1016/S0960-9822(02)00791-1.

74. Fukumoto A, Tomoda K, Kubota M, Kato JY, Yoneda-Kato N. 2005. Small Jab1-containing subcomplex is regulated in an anchorage- and cell cycle-dependent manner, which is abrogated by ras transformation. FEBS Lett 579:1047–1054. https://doi.org/10.1016/j.febslet.2004.12.076.

75. Dornan D, Shimizu H, Mah A, Dudhela T, Eby M, O'Rourke K, Seshagiri S, Dixit VM. 2006. ATM engages autodegradation of the E3 ubiquitin ligase COP1 after DNA damage. Science 313:1122–1126. https://doi.org/10.1126/science.1127335.

76. Higa LA, Mihaylov IS, Banks DP, Zheng J, Zhang H. 2003. Radiation-mediated proteolysis of CDT1 by CUL4-ROC1 and CSN complexes constitutes a new checkpoint. Nat Cell Biol 5:1008–1015. https://doi.org/10.1038/ncb1061.

77. Huang J, Yuan H, Lu C, Liu X, Cao X, Wan M. 2007. Jab1 mediates protein degradation of the Rad9-Rad1-Hus1 checkpoint complex. J Mol Biol 371:514–527. https://doi.org/10.1016/j.jmb.2007.05.095.

78. Matsuoka S, Ballif BA, Smogorzewska A, McDonald ER, III, Hurov KE, Luo J, Bakalarski CE, Zhao Z, Solimini N, Lerenthal Y, Shiloh Y, Gygi SP, Elledge SJ. 2007. ATM and ATR substrate analysis reveals extensive protein networks responsive to DNA damage. Science 316:1160–1166. https://doi.org/10.1126/science.1140321.

79. da Silva Correia J, Miranda Y, Leonard N, Ulevitch RJ. 2007. The subunit CSN6 of the COP9 signalosome is cleaved during apoptosis. J Biol Chem 282:12557–12565. https://doi.org/10.1074/jbc.M609587200.

80. Hetfeld BK, Peth A, Sun XM, Henklein P, Cohen GM, Dubiel W. 2008. The COP9 signalosome-mediated deneddylation is stimulated by caspases during apoptosis. Apoptosis 13:187–195. https://doi.org/10.1007/s10495-007-0164-7.

81. Pearce C, Hayden RE, Bunce CM, Khanim FL. 2009. Analysis of the role of COP9 signalosome (CSN) subunits in K562; the first link between CSN and autophagy. BMC Cell Biol 10:31. https://doi.org/10.1186/1471-2121-10-31.

82. Lee MH, Zhao R, Phan L, Yeung SC. 2011. Roles of COP9 signalosome in cancer. Cell Cycle 10:3057–3066. https://doi.org/10.4161/cc.10.18.17320.

83. Zhao R, Yeung SC, Chen J, Iwakuma T, Su CH, Chen B, Qu C, Zhang F, Chen YT, Lin YL, Lee DF, Jin F, Zhu R, Shaikenov T, Sarbassov D, Sahin A, Wang H, Lai CC, Tsai FJ, Lozano G, Lee MH. 2011. Subunit 6 of the COP9 signalosome promotes tumorigenesis in mice through stabilization of MDM2 and is upregulated in human cancers. J Clin Invest 121:851–865. https://doi.org/10.1172/JCI44111.

84. Deng Z, Pardi R, Cheadle W, Xiang X, Zhang S, Shah SV, Grizzle W, Miller D, Mountz J, Zhang HG. 2011. Plant homologue constitutive photomorphogenesis 9 (COP9) signalosome subunit CSN5 regulates innate immune responses in macrophages. Blood 117:4796–4804. https://doi.org/10.1182/blood-2010-10-314526.

85. Kurnellas MP, Li H, Jain MR, Giraud SN, Nicot AB, Ratnayake A, Heary RF, Elkabes S. 2010. Reduced expression of plasma membrane calcium ATPase 2 and collapsin response mediator protein 1 promotes death of spinal cord neurons. Cell Death Differ 17:1501–1510. https://doi.org/10.1038/cdd.2010.54.

86. Stone RC, Du P, Feng D, Dhawan K, Rönnblom L, Eloranta ML, Donnelly R, Barnes BJ. 2013. RNA-Seq for enrichment and analysis of IRF5 transcript expression in SLE. PLoS One 8:e54487. https://doi.org/10.1371/journal.pone.0054487.